

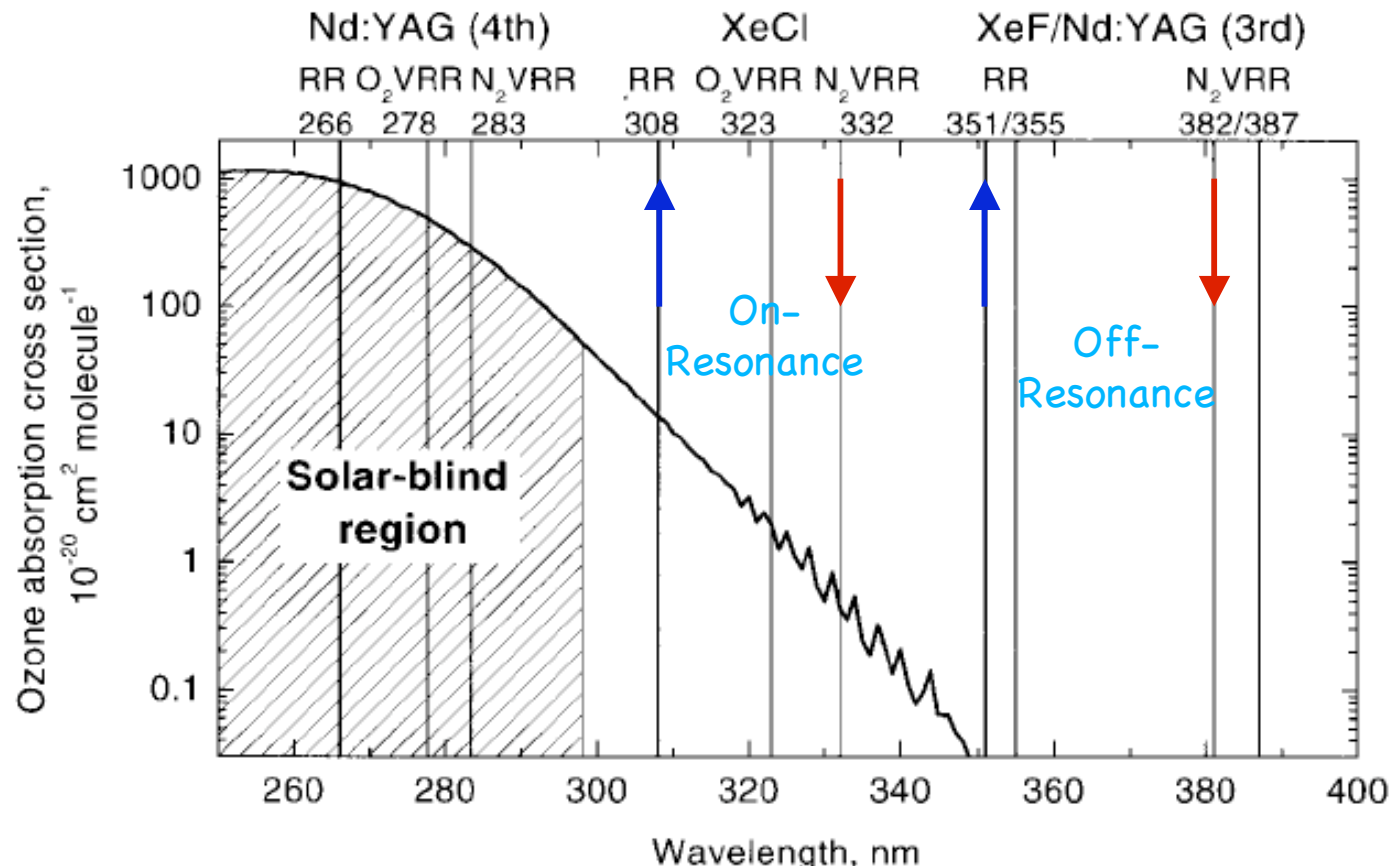
# Lecture 29A. Constituent Lidar (3)

- ❑ Conventional Raman DIAL vs. RVR Raman DIAL
- ❑ Multiwavelength DIAL
- ❑ Comparison of Constituent Lidar Techniques
- ❑ Summary for DIAL and Raman

# Lecture 29B. Target Lidar

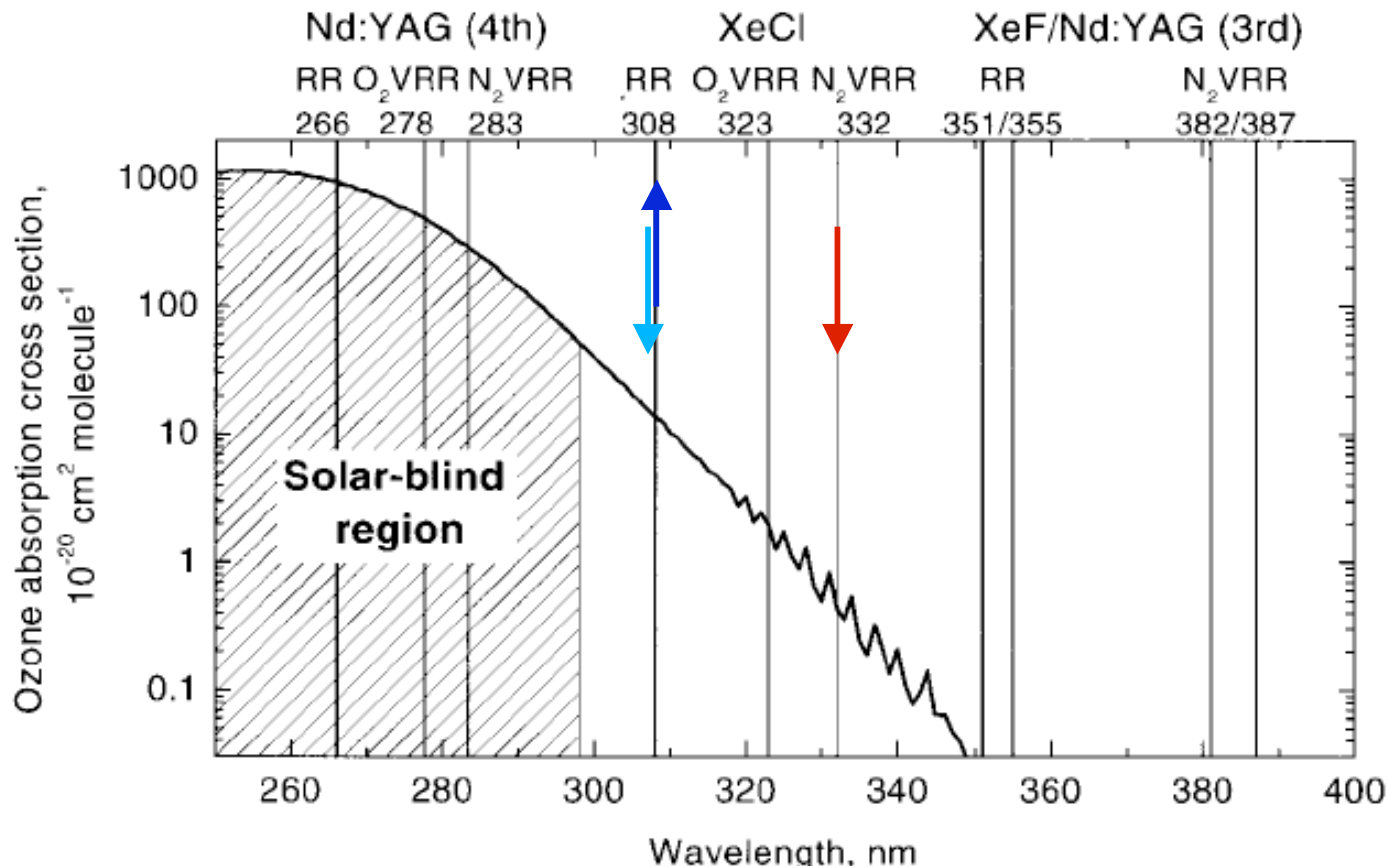
- ❑ Motivations for Target Lidar
- ❑ Laser Altimeter
- ❑ GLAS on ICESat
- ❑ Fluorescence Lidar for Liquids and Solids
- ❑ More Target and Imaging Lidars
- ❑ Summary of Target Lidar Techniques

# Raman DIAL versus RVR Raman DIAL for O<sub>3</sub> Measurements in Clouds



Conventional Raman DIAL uses two primary wavelengths transmitted (e.g., 308 and 351 nm) into the atmosphere and ozone calculated from the differential absorption of the corresponding Raman return signals of molecular N<sub>2</sub> (e.g., 332 and 382 nm).

# RVR Raman DIAL for Ozone



Rotational Vibrational-Rotational Raman DIAL transmits single primary wavelength (e.g., 308 nm) into the atmosphere and ozone measurement is based on differential absorption of ozone between the purely rotational Raman (RR) return signals from N<sub>2</sub> (307 nm) and O<sub>2</sub> (307 nm) as the on-resonance wavelength, and the vibrational-rotational Raman (VRR) return signals from N<sub>2</sub> (332 nm) or O<sub>2</sub> (323 nm) as the off-resonance wavelength.

# RVR Raman DIAL

Table 1. Parameters of the Conventional Raman DIAL and the RVR Raman DIAL's<sup>a</sup>

Lidar	On-Resonance		Off-Resonance			$\Delta C_{O_3}^{abs}$ ( $10^{-24} \text{ m}^2$ )
	Raman Wavelength (nm)	$\lambda_L$ (nm)	Raman Wavelength (nm)	$\lambda_L$ (nm)	$\Delta\lambda$ (nm)	
O <sub>2</sub> RVR Raman DIAL	307	308	323	308	16	11.7
N <sub>2</sub> RVR Raman DIAL	307	308	332	308	25	12.3
Raman DIAL	332	308	387	355	79	12.4

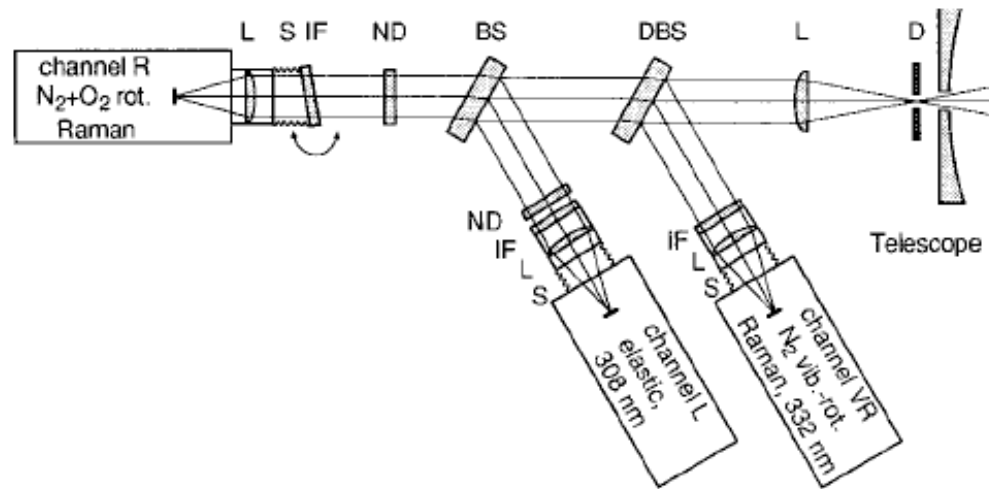


Fig. 3. RVR Raman DIAL receiver: D, diaphragm; L, lens; DBS, dichroic beam splitter; BS, beam splitter; ND, neutral-density filter; IF, interference filter; S, flexible shield. Atmospheric rotational Raman, elastic, and N<sub>2</sub> vibrational-rotational Raman backscattering signals are detected in channels R, L, and VR. The center wavelength of the channel-R interference filter can be tuned by rotating the filter around the vertical axis.

# RVR Raman DIAL Equation

- For the elastic DIAL channel at ON-resonance wavelength 308 nm,

$$P_S(\lambda_L, R) = P_L(\lambda_L) \left[ (\beta_{aer}(\lambda_L, R) + \beta_{mol}(\lambda_L, R)) \Delta R \right] \left( \frac{A}{R^2} \right) \exp \left[ -2 \int_0^R (\alpha_{aer}(\lambda_L, r) + \alpha_{mol}(\lambda_L, r)) dr \right] \\ \times \exp \left[ -2 \int_0^R \sigma_{IG}(\lambda_L, r) n_{IG} dr \right] \exp \left[ -2 \int_0^R \sigma_{abs}(\lambda_L, r) n_c(r) dr \right] \left[ \eta(\lambda_L) G(R) \right] + P_B$$

- For the purely rotational Raman channels from N<sub>2</sub> and O<sub>2</sub> at 307 nm,

$$P_S(\lambda_{RR}, R) = P_L(\lambda_L) \left[ \beta_{Raman}(\lambda_{RR}, R) \Delta R \right] \left( \frac{A}{R^2} \right) \\ \times \exp \left[ - \int_0^R (\alpha_{aer}(\lambda_L, r) + \alpha_{aer}(\lambda_{RR}, r) + \alpha_{mol}(\lambda_L, r) + \alpha_{mol}(\lambda_{RR}, r)) dr \right] \\ \times \exp \left[ - \int_0^R (\sigma_{IG}(\lambda_L, r) + \sigma_{IG}(\lambda_{RR}, r)) n_{IG} dr \right] \\ \times \exp \left[ - \int_0^R (\sigma_{abs}(\lambda_L, r) + \sigma_{abs}(\lambda_{RR}, r)) n_c(r) dr \right] \left[ \eta(\lambda_{RR}) G(R) \right] + P_B$$

The beauty of the RVR Raman DIAL is the utilization of pure rotational Raman (RR) scattering so that aerosol backscatter is excluded in the RR channel.

# RVR Raman DIAL Equation Cont'd

□ For the vibrational-rotational Raman channel from N<sub>2</sub> at 332 nm,

$$P_S(\lambda_{VRR}, R) = P_L(\lambda_L) \left[ \beta_{Raman}(\lambda_{VRR}, R) \Delta R \right] \left( \frac{A}{R^2} \right) \\ \times \exp \left[ - \int_0^R \left( \alpha_{aer}(\lambda_L, r) + \alpha_{aer}(\lambda_{VRR}, r) + \alpha_{mol}(\lambda_L, r) + \alpha_{mol}(\lambda_{VRR}, r) \right) dr \right] \\ \times \exp \left[ - \int_0^R \left( \sigma_{IG}(\lambda_L, r) + \sigma_{IG}(\lambda_{VRR}, r) \right) n_{IG} dr \right] \\ \times \exp \left[ - \int_0^R \left( \sigma_{abs}(\lambda_L, r) + \sigma_{abs}(\lambda_{VRR}, r) \right) n_c(r) dr \right] \left[ \eta(\lambda_{VRR}) G(R) \right] + P_B$$

Certainly, the vibrational-rotational Raman (VRR) scattering channel also excludes aerosol backscatter.

# Solution for RVR Raman DIAL

From the Rotational Raman (RR) and the Vibrational-Rotational Raman (VRR) equations, the ozone number density can be derived as

$$n_c(R) = \frac{1}{\Delta\sigma_{abs}} \frac{d}{dR} \left\{ \begin{array}{l} \ln \left[ \frac{P_S(\lambda_{VRR}, R) - P_B}{P_S(\lambda_{RR}, R) - P_B} \right] \\ - \ln \left[ \frac{\eta(\lambda_{VRR})}{\eta(\lambda_{RR})} \right] \\ - \ln \left[ \frac{\beta_{Raman}(\lambda_{VRR}, R)}{\beta_{Raman}(\lambda_{RR}, R)} \right] \\ - \Delta\alpha_{aer}(R) \\ - \Delta\alpha_{mol}(R) \\ - \Delta\sigma_{IG}(R)n_{IG} \end{array} \right\} \begin{array}{l} \text{---} \\ \text{---} \\ \text{---} \\ \text{---} \\ \text{---} \\ \text{---} \end{array} \begin{array}{l} \text{A} \\ \text{B} \\ \text{C} \\ \text{D} \\ \text{E} \\ \text{F} \end{array}$$

Here, the  $\Delta$  expressions consist of four terms each

$$\Delta\xi = \xi(\lambda_{RR}) - \xi(\lambda_{VRR})$$

with

$$\xi = \sigma_{abs}, \alpha_{aer}, \alpha_{mol}, \sigma_{IG}$$

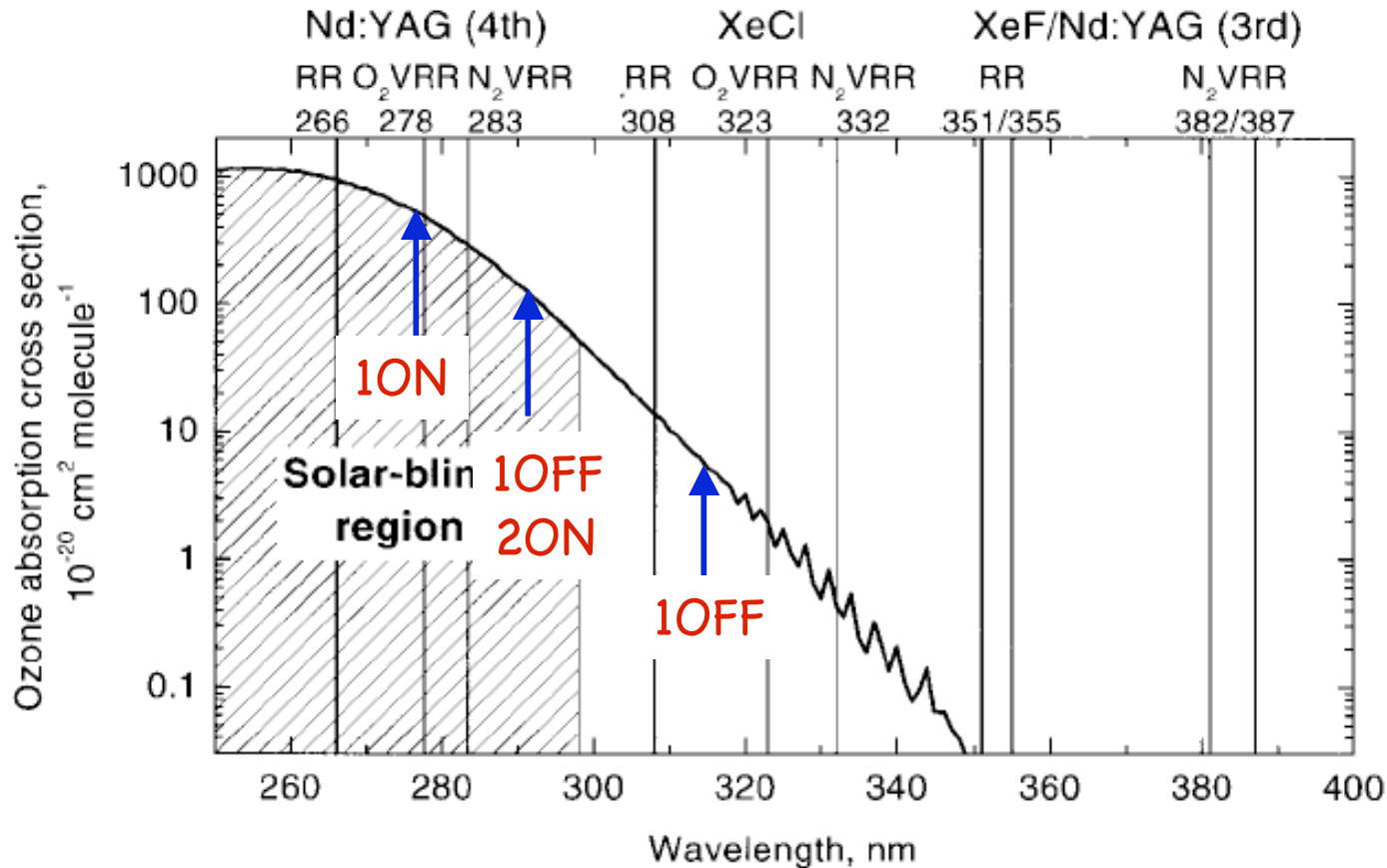
# Challenge in RVR Raman DIAL

- ❑ Term B is range-independent, so the derivative is zero,
- ❑ Term C is only concerned about molecule Raman scattering.
- ❑ Term D will be determined through using the Raman VRR channel and introducing Angstrom exponent.
- ❑ Term E is concerned about molecule Rayleigh scattering, so can be calculated from atmosphere temperature and pressure.
- ❑ Term F can be minimized through choosing proper wavelengths, thus, can be ignored.

The main challenge in RVR Raman DIAL is how to sufficiently suppress the elastic scattering at laser wavelength in the pure rotational Raman (RR) channel, as the wavelength difference is only 1 nm.

Modern interference filter has FWHM of 0.3 nm, but its wing (or tail) can certainly extend to more than 1 nm. Since Rayleigh scattering is about 3 orders of magnitude larger than rotational Raman scattering, the influence from Rayleigh scattering is not easy to be excluded.  
Thus, RVR Raman DIAL is not easy to be realized.

# Multiwavelength DIAL



Multiwavelength DIAL uses three or more wavelengths transmitted into the atmosphere and ozone calculated from the differential absorption of several pairs of elastic scattering signals from air molecules and aerosols. The influence from differential scattering and extinction of aerosols are dramatically decreased by properly choosing wavelengths.

# Multiwavelength DIAL Equation

□ For the elastic DIAL channel at 1ON-resonance wavelength,

$$P_S(\lambda_1^{ON}, R) = P_L(\lambda_1^{ON}) \left[ \left( \beta_{aer}(\lambda_1^{ON}, R) + \beta_{mol}(\lambda_1^{ON}, R) \right) \Delta R \right] \left( \frac{A}{R^2} \right) \exp \left[ -2 \int_0^R \left( \alpha_{aer}(\lambda_1^{ON}, r) + \alpha_{mol}(\lambda_1^{ON}, r) \right) dr \right] \\ \times \exp \left[ -2 \int_0^R \sigma_{IG}(\lambda_1^{ON}, r) n_{IG}(r) dr \right] \exp \left[ -2 \int_0^R \sigma_{abs}(\lambda_1^{ON}, r) n_c(r) dr \right] \left[ \eta(\lambda_1^{ON}) G(R) \right] + P_B$$

□ For the elastic DIAL channel at 1OFF-resonance wavelength,

$$P_S(\lambda_1^{OFF}, R) = P_L(\lambda_1^{OFF}) \left[ \left( \beta_{aer}(\lambda_1^{OFF}, R) + \beta_{mol}(\lambda_1^{OFF}, R) \right) \Delta R \right] \left( \frac{A}{R^2} \right) \exp \left[ -2 \int_0^R \left( \alpha_{aer}(\lambda_1^{OFF}, r) + \alpha_{mol}(\lambda_1^{OFF}, r) \right) dr \right] \\ \times \exp \left[ -2 \int_0^R \sigma_{IG}(\lambda_1^{OFF}, r) n_{IG}(r) dr \right] \exp \left[ -2 \int_0^R \sigma_{abs}(\lambda_1^{OFF}, r) n_c(r) dr \right] \left[ \eta(\lambda_1^{OFF}) G(R) \right] + P_B$$

□ For the elastic DIAL channel at 2ON-resonance wavelength,

$$P_S(\lambda_2^{ON}, R) = P_L(\lambda_2^{ON}) \left[ \left( \beta_{aer}(\lambda_2^{ON}, R) + \beta_{mol}(\lambda_2^{ON}, R) \right) \Delta R \right] \left( \frac{A}{R^2} \right) \exp \left[ -2 \int_0^R \left( \alpha_{aer}(\lambda_2^{ON}, r) + \alpha_{mol}(\lambda_2^{ON}, r) \right) dr \right] \\ \times \exp \left[ -2 \int_0^R \sigma_{IG}(\lambda_2^{ON}, r) n_{IG}(r) dr \right] \exp \left[ -2 \int_0^R \sigma_{abs}(\lambda_2^{ON}, r) n_c(r) dr \right] \left[ \eta(\lambda_2^{ON}) G(R) \right] + P_B$$

□ For the elastic DIAL channel at 2OFF-resonance wavelength,

$$P_S(\lambda_2^{OFF}, R) = P_L(\lambda_2^{OFF}) \left[ \left( \beta_{aer}(\lambda_2^{OFF}, R) + \beta_{mol}(\lambda_2^{OFF}, R) \right) \Delta R \right] \left( \frac{A}{R^2} \right) \exp \left[ -2 \int_0^R \left( \alpha_{aer}(\lambda_2^{OFF}, r) + \alpha_{mol}(\lambda_2^{OFF}, r) \right) dr \right] \\ \times \exp \left[ -2 \int_0^R \sigma_{IG}(\lambda_2^{OFF}, r) n_{IG}(r) dr \right] \exp \left[ -2 \int_0^R \sigma_{abs}(\lambda_2^{OFF}, r) n_c(r) dr \right] \left[ \eta(\lambda_2^{OFF}) G(R) \right] + P_B$$

# 3-Wavelength Dual-DIAL for O<sub>3</sub>

□ From above equations, we can derive the following

$$\begin{aligned}
 \ln\left(\frac{P_S(\lambda_1^{ON}, R) - P_B}{P_S(\lambda_1^{OFF}, R) - P_B} \bigg/ \frac{P_S(\lambda_2^{ON}, R) - P_B}{P_S(\lambda_2^{OFF}, R) - P_B}\right) &= \ln\left(\frac{P_L(\lambda_1^{ON})\eta(\lambda_1^{ON})}{P_L(\lambda_1^{OFF})\eta(\lambda_1^{OFF})} \bigg/ \frac{P_L(\lambda_2^{ON})\eta(\lambda_2^{ON})}{P_L(\lambda_2^{OFF})\eta(\lambda_2^{OFF})}\right) \\
 &+ \ln\left(\frac{\beta_{aer}(\lambda_1^{ON}, R) + \beta_{mol}(\lambda_1^{ON}, R)}{\beta_{aer}(\lambda_1^{OFF}, R) + \beta_{mol}(\lambda_1^{OFF}, R)} \bigg/ \frac{\beta_{aer}(\lambda_2^{ON}, R) + \beta_{mol}(\lambda_2^{ON}, R)}{\beta_{aer}(\lambda_2^{OFF}, R) + \beta_{mol}(\lambda_2^{OFF}, R)}\right) \\
 &- 2 \int_0^R \left[ \left( \alpha_{aer}(\lambda_1^{ON}, r) - \alpha_{aer}(\lambda_1^{OFF}, r) \right) - \left( \alpha_{aer}(\lambda_2^{ON}, r) - \alpha_{aer}(\lambda_2^{OFF}, r) \right) \right] dr \\
 &- 2 \int_0^R \left[ \left( \alpha_{mol}(\lambda_1^{ON}, r) - \alpha_{mol}(\lambda_1^{OFF}, r) \right) - \left( \alpha_{mol}(\lambda_2^{ON}, r) - \alpha_{mol}(\lambda_2^{OFF}, r) \right) \right] dr \\
 &- 2 \int_0^R \left[ \left( \sigma_{IG}(\lambda_1^{ON}, r) - \sigma_{IG}(\lambda_1^{OFF}, r) \right) - \left( \sigma_{IG}(\lambda_2^{ON}, r) - \sigma_{IG}(\lambda_2^{OFF}, r) \right) \right] n_{IG}(r) dr \\
 &- 2 \int_0^R \left[ \left( \sigma_{abs}(\lambda_1^{ON}, r) - \sigma_{abs}(\lambda_1^{OFF}, r) \right) - \left( \sigma_{abs}(\lambda_2^{ON}, r) - \sigma_{abs}(\lambda_2^{OFF}, r) \right) \right] n_c(r) dr
 \end{aligned}$$

Three wavelengths form a dual-pair DIAL, with  $\lambda_{1OFF} = \lambda_{2ON}$ . Thus, the influence from aerosol extinction and backscatter can be minimized by choosing appropriate pairs of wavelengths.

# Solution for Dual-DIAL $O_3$

□ Ozone number density can be derived from above equations:

$$n_c(R) = \frac{1}{2\Delta\sigma_{abs}} \frac{d}{dR} \left\{ \begin{array}{l} -\ln\left(\frac{P_S(\lambda_1^{ON}, R) - P_B}{P_S(\lambda_1^{OFF}, R) - P_B} \bigg/ \frac{P_S(\lambda_2^{ON}, R) - P_B}{P_S(\lambda_2^{OFF}, R) - P_B}\right) \\ +\ln\left(\frac{P_L(\lambda_1^{ON})\eta(\lambda_1^{ON})}{P_L(\lambda_1^{OFF})\eta(\lambda_1^{OFF})} \bigg/ \frac{P_L(\lambda_2^{ON})\eta(\lambda_2^{ON})}{P_L(\lambda_2^{OFF})\eta(\lambda_2^{OFF})}\right) \\ +\left[\ln\left(\frac{\beta_{aer}(\lambda_1^{ON}, R) + \beta_{mol}(\lambda_1^{ON}, R)}{\beta_{aer}(\lambda_1^{OFF}, R) + \beta_{mol}(\lambda_1^{OFF}, R)}\right) - \ln\left(\frac{\beta_{aer}(\lambda_2^{ON}, R) + \beta_{mol}(\lambda_2^{ON}, R)}{\beta_{aer}(\lambda_2^{OFF}, R) + \beta_{mol}(\lambda_2^{OFF}, R)}\right)\right] \\ -\left[\left(\alpha_{aer}(\lambda_1^{ON}, R) - \alpha_{aer}(\lambda_1^{OFF}, R)\right) - \left(\alpha_{aer}(\lambda_2^{ON}, R) - \alpha_{aer}(\lambda_2^{OFF}, R)\right)\right] \\ -\left[\left(\alpha_{mol}(\lambda_1^{ON}, R) - \alpha_{mol}(\lambda_1^{OFF}, R)\right) - \left(\alpha_{mol}(\lambda_2^{ON}, R) - \alpha_{mol}(\lambda_2^{OFF}, R)\right)\right] \\ -\left[\left(\sigma_{IG}(\lambda_1^{ON}, R) - \sigma_{IG}(\lambda_1^{OFF}, R)\right) - \left(\sigma_{IG}(\lambda_2^{ON}, R) - \sigma_{IG}(\lambda_2^{OFF}, R)\right)\right]n_{IG}(R) \end{array} \right\} \begin{array}{l} \text{--- A} \\ \text{--- B} \\ \text{--- C} \\ \text{--- D} \\ \text{--- E} \\ \text{--- F} \end{array}$$

Where the differential absorption cross-section is defined as

$$\Delta\sigma_{abs} = \left(\sigma_{abs}(\lambda_1^{ON}, r) - \sigma_{abs}(\lambda_1^{OFF}, r)\right) - \left(\sigma_{abs}(\lambda_2^{ON}, r) - \sigma_{abs}(\lambda_2^{OFF}, r)\right)$$

# Choice of Wavelength for Dual-DIAL

$$\Delta\beta = \ln\left(\frac{\beta_{aer}(\lambda_1^{ON}, R) + \beta_{mol}(\lambda_1^{ON}, R)}{\beta_{aer}(\lambda_1^{OFF}, R) + \beta_{mol}(\lambda_1^{OFF}, R)}\right) - \ln\left(\frac{\beta_{aer}(\lambda_2^{ON}, R) + \beta_{mol}(\lambda_2^{ON}, R)}{\beta_{aer}(\lambda_2^{OFF}, R) + \beta_{mol}(\lambda_2^{OFF}, R)}\right)$$

$$\Delta\alpha_{aer} = \left(\alpha_{aer}(\lambda_1^{ON}, R) - \alpha_{aer}(\lambda_1^{OFF}, R)\right) - \left(\alpha_{aer}(\lambda_2^{ON}, R) - \alpha_{aer}(\lambda_2^{OFF}, R)\right)$$

$$\Delta\alpha_{mol} = \left(\alpha_{mol}(\lambda_1^{ON}, R) - \alpha_{mol}(\lambda_1^{OFF}, R)\right) - \left(\alpha_{mol}(\lambda_2^{ON}, R) - \alpha_{mol}(\lambda_2^{OFF}, R)\right)$$

$$\Delta\sigma_{IG} = \left(\sigma_{IG}(\lambda_1^{ON}, R) - \sigma_{IG}(\lambda_1^{OFF}, R)\right) - \left(\sigma_{IG}(\lambda_2^{ON}, R) - \sigma_{IG}(\lambda_2^{OFF}, R)\right)$$

$$\Delta\sigma_{abs} = \left(\sigma_{abs}(\lambda_1^{ON}, r) - \sigma_{abs}(\lambda_1^{OFF}, r)\right) - \left(\sigma_{abs}(\lambda_2^{ON}, r) - \sigma_{abs}(\lambda_2^{OFF}, r)\right)$$

❑ Different channels interact on the same aerosols and interference gases (IG) but with different wavelengths. The main error in conventional DIAL is caused by the uncertainty of the wavelength dependence and information (like density) of the backscatter, extinction, and interference owing to aerosols and IG.

$$\beta_{aer}(\lambda) \propto \frac{1}{\lambda^a}, \quad \alpha_{aer}(\lambda) \propto \frac{1}{\lambda^a}$$

❑ If the wavelength dependence (Angstrom factor) is stable within the detection wavelength range, it is possible to cancel the influence by carefully choosing the wavelengths of two pairs - the difference between two pairs can be minimized.

# Solution for Dual-DIAL $O_3$

- ❑ By choosing the pairs of wavelengths, terms C-F (now the difference at two pairs of DIAL wavelengths) can be minimized or cancelled out. Thus, the  $O_3$  measurement errors caused by the uncertainties of terms C-F can be dramatically decreased.
- ❑ Notice that the choice of the pairs of wavelengths must satisfy one important condition that the differential absorption cross-section given above must be large enough to meet the requirements of measurements sensitivity and spatial resolution.
- ❑ For the  $O_3$  measurements, the dual-DIAL can be carried out by three wavelengths chosen at 277.1, 291.8, and 313.2 nm. The middle wavelength 291.8 nm acts as the off-wavelength for the 1st pair, while the on-wavelength for the 2nd pair.
- ❑ To minimize the influence from aerosol backscatter and extinction, a constant C can be introduced into above lidar equation. C is approximately determined by the ratio of the wavelength differences between two pairs of DIAL:

$$C = \frac{\lambda_1^{ON} - \lambda_1^{OFF}}{\lambda_2^{ON} - \lambda_2^{OFF}}$$

Here  $\lambda_1^{OFF} = \lambda_2^{ON}$

# Solution with Constant C Introduced

$$n_c(R) = \frac{1}{2\Delta\sigma_{abs}} \frac{d}{dR} \left\{ \begin{array}{l} \text{--- A ---} \\ -\ln \left( \frac{P_S(\lambda_1^{ON}, R) - P_B}{P_S(\lambda_1^{OFF}, R) - P_B} \middle/ \left( \frac{P_S(\lambda_2^{ON}, R) - P_B}{P_S(\lambda_2^{OFF}, R) - P_B} \right)^C \right) \\ \text{--- B ---} \\ +\ln \left( \frac{P_L(\lambda_1^{ON})\eta(\lambda_1^{ON})}{P_L(\lambda_1^{OFF})\eta(\lambda_1^{OFF})} \middle/ \left( \frac{P_L(\lambda_2^{ON})\eta(\lambda_2^{ON})}{P_L(\lambda_2^{OFF})\eta(\lambda_2^{OFF})} \right)^C \right) \\ \text{--- C ---} \\ + \left[ \ln \left( \frac{\beta_{aer}(\lambda_1^{ON}, R) + \beta_{mol}(\lambda_1^{ON}, R)}{\beta_{aer}(\lambda_1^{OFF}, R) + \beta_{mol}(\lambda_1^{OFF}, R)} \right) - C \ln \left( \frac{\beta_{aer}(\lambda_2^{ON}, R) + \beta_{mol}(\lambda_2^{ON}, R)}{\beta_{aer}(\lambda_2^{OFF}, R) + \beta_{mol}(\lambda_2^{OFF}, R)} \right) \right] \\ \text{--- D ---} \\ - \left[ \left( \alpha_{aer}(\lambda_1^{ON}, R) - \alpha_{aer}(\lambda_1^{OFF}, R) \right) - C \left( \alpha_{aer}(\lambda_2^{ON}, R) - \alpha_{aer}(\lambda_2^{OFF}, R) \right) \right] \\ \text{--- E ---} \\ - \left[ \left( \alpha_{mol}(\lambda_1^{ON}, R) - \alpha_{mol}(\lambda_1^{OFF}, R) \right) - C \left( \alpha_{mol}(\lambda_2^{ON}, R) - \alpha_{mol}(\lambda_2^{OFF}, R) \right) \right] \\ \text{--- F ---} \\ - \left[ \left( \sigma_{IG}(\lambda_1^{ON}, R) - \sigma_{IG}(\lambda_1^{OFF}, R) \right) - C \left( \sigma_{IG}(\lambda_2^{ON}, R) - \sigma_{IG}(\lambda_2^{OFF}, R) \right) \right] n_{IG}(R) \end{array} \right\}$$

Where the differential absorption cross-section is defined as

$$\Delta\sigma_{abs} = \left( \sigma_{abs}(\lambda_1^{ON}, r) - \sigma_{abs}(\lambda_1^{OFF}, r) \right) - C \left( \sigma_{abs}(\lambda_2^{ON}, r) - \sigma_{abs}(\lambda_2^{OFF}, r) \right)$$

# Simulation Results for Dual-DIAL O<sub>3</sub>

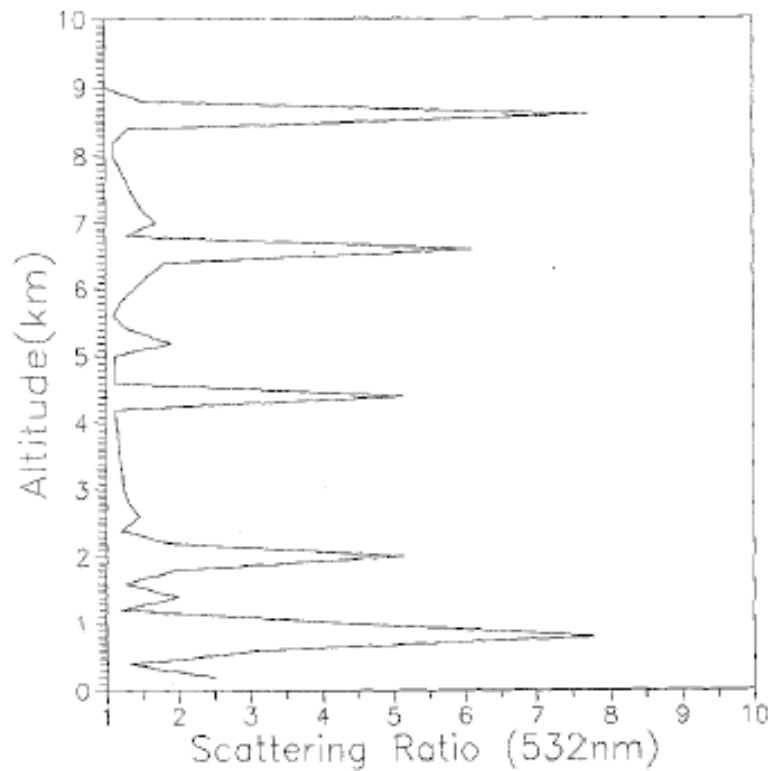


Fig. 1. Profile of the aerosol scattering ratio (532 nm)

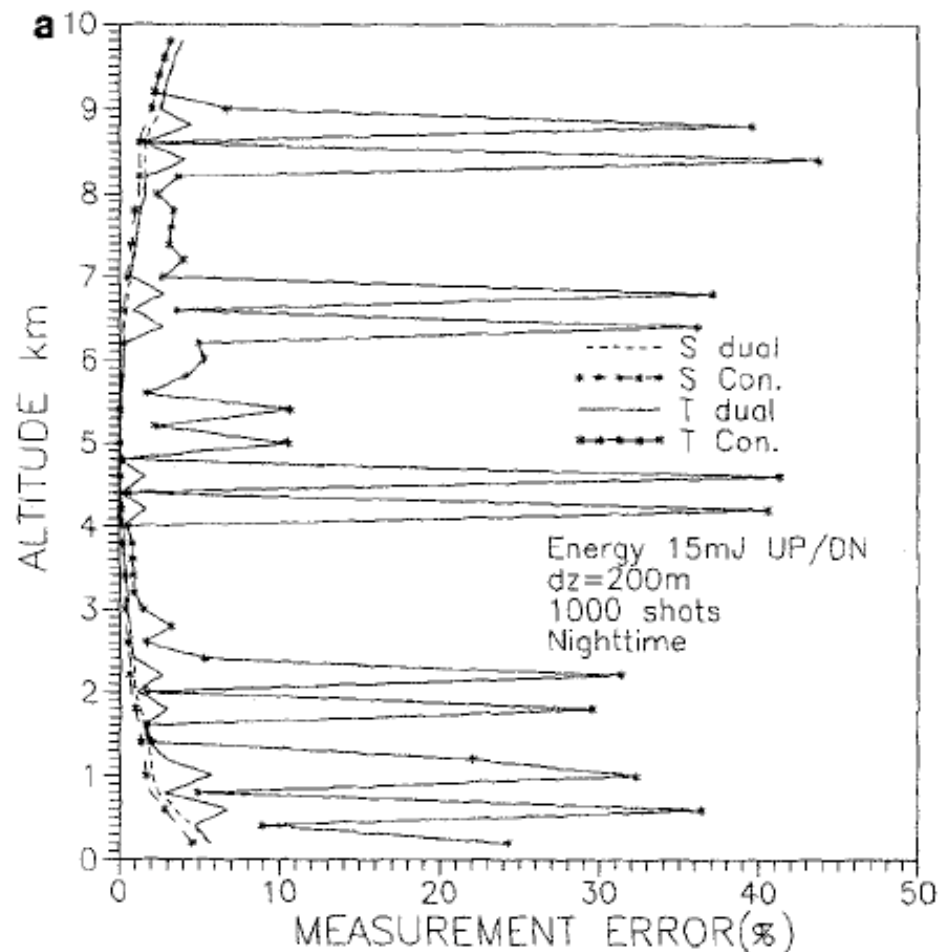
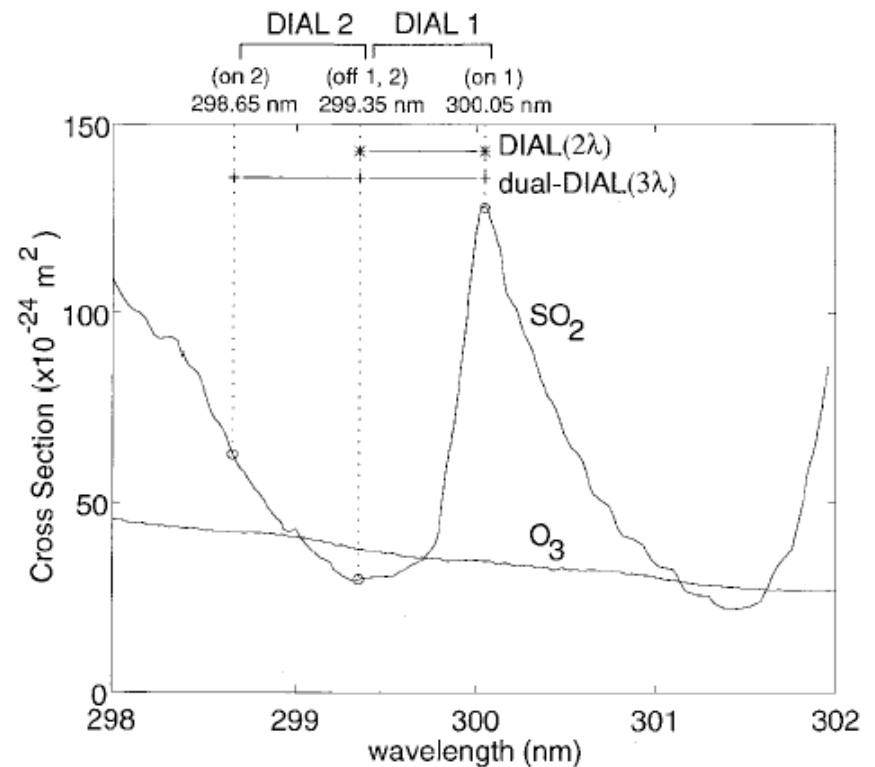
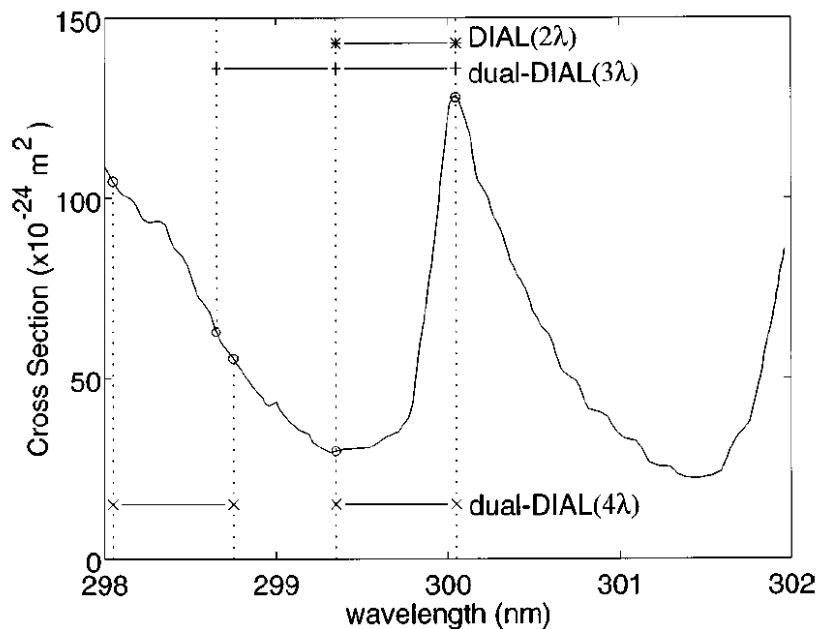


Fig. 2a, b. Simulations of measurement error vs altitude for the dual-DIAL with 277.1, 291.8, 313.2 nm and conventional DIAL with 277.1, 291.8 nm operated from an aircraft flying at an altitude of 5 km. The ozone profile is the US standard ozone profile. In the legend, *S* represents the statistical error, *T* the total measurement error, *dual* the dual-DIAL method and *con.* the conventional DIAL method: (a) night-time; (b) day-time

$$C = 0.65$$

# Dual-DIAL for SO<sub>2</sub> Measurements



**Fig. 1** Absorption cross section of SO<sub>2</sub>. The wavelengths used in two-wavelength DIAL, three-wavelength dual-DIAL, and four-wavelength dual-DIAL are indicated.

**Fig. 1.** Wavelengths used in three-wavelength dual DIAL for SO<sub>2</sub>, and absorption cross sections of SO<sub>2</sub> and O<sub>3</sub>.

Fukuchi et al., Opt. Eng., 1999  
 Fujii et al., Applied Optics, 2001

# Dual-DIAL for SO<sub>2</sub> Measurements

**Table 1** Cases considered for SO<sub>2</sub> measurement.  $n\sigma'$  and  $n\sigma''$  are given for a SO<sub>2</sub> concentration of 1 ppb.

Method	$\sigma'_0, \sigma''_0$ (10 <sup>-24</sup> m <sup>2</sup> )	$n\sigma'_0, n\sigma''_0$ (10 <sup>-6</sup> m <sup>-1</sup> )	$\alpha'_x, \alpha''_x$ (10 <sup>-6</sup> m <sup>-1</sup> )	$i$	$\lambda_i$ (nm)	$e_i$	
DIAL	98.0	2.5	-3.7	1	299.35	-1 <sup>a</sup>	
				2	300.05	+1 <sup>b</sup>	
Dual-DIAL:							
3-wavelength	131	3.3	0.83	1	298.65	+1	
				2	299.35	-1	
				3			
				4			300.05
4-wavelength	148	3.8	0.094	1	298.05	+1	
				2	298.75	-1	
				3			299.35
				4			

<sup>a</sup>Off.

<sup>b</sup>On.

$$n = \frac{1}{2 \Delta R \sigma''_0} \left[ \sum_{i=1}^m e_i Z(R, \lambda_i) - \sum_{i=1}^m e_i B(R, \lambda_i) \right] - \frac{\alpha''_x}{\sigma''_0}$$

$$\sigma''_0 = \sum_{i=1}^m e_i \sigma_0(\lambda_i)$$

$$\alpha''_x = \sum_{i=1}^m e_i \alpha_x(\lambda_i)$$

# Comparison of Constituent Lidar Tech

Technique	Signal Source & Trace Gas		Interests
Resonance Fluorescence Lidar	Resonance fluorescence from metal atoms in middle and upper atmosphere		Temp, Wind, Density, Wave
Resonance Fluorescence Lidar	Resonance fluorescence from He, N <sub>2</sub> <sup>+</sup> , O in thermosphere		Density, Temp Wind, etc
Conventional DIAL	Elastic-scattering from air molecules and aerosols	Trace gas absorption in the extinction terms	Species, Density
Raman Lidar	Inelastic Raman scattering from trace gas and reference N <sub>2</sub> or O <sub>2</sub>	Trace gas scattering in the backscatter terms (no aerosol scattering)	Species, Density, Mixing ratio
Raman DIAL	Inelastic Raman scattering from N <sub>2</sub> or O <sub>2</sub>	Trace gas absorption in the extinction terms	Species, Density
RVR Raman DIAL	Pure rotational Raman scattering and Vibrational-Rotational Raman scattering	Trace gas absorption in the extinction terms	Species, Density
Multiwavelength DIAL	Elastic scattering from air molecules and aerosols	Trace gas absorption in the extinction terms	Species, Density

Range-Resolved spatial & temporal distribution of these species, density, temp, wind and waves

# Backscatter Cross-Section Comparison

Physical Process	Backscatter Cross-Section	Mechanism
Mie (Aerosol) Scattering	$10^{-8} - 10^{-10} \text{ cm}^2\text{sr}^{-1}$	Two-photo process Elastic scattering, instantaneous
Resonance Fluorescence	$10^{-13} \text{ cm}^2\text{sr}^{-1}$	Two single-photo process (absorption and spontaneous emission) Delayed (radiative lifetime)
Molecular Absorption	$10^{-19} \text{ cm}^2\text{sr}^{-1}$	Single-photon process
Fluorescence from molecule, liquid, solid	$10^{-19} \text{ cm}^2\text{sr}^{-1}$	Two single-photon process Inelastic scattering, delayed (lifetime)
Rayleigh Scattering	$10^{-27} \text{ cm}^2\text{sr}^{-1}$	Two-photon process Elastic scattering, instantaneous
Raman Scattering	$10^{-30} \text{ cm}^2\text{sr}^{-1}$	Two-photon process Inelastic scattering, instantaneous

# Summary for DIAL and Raman

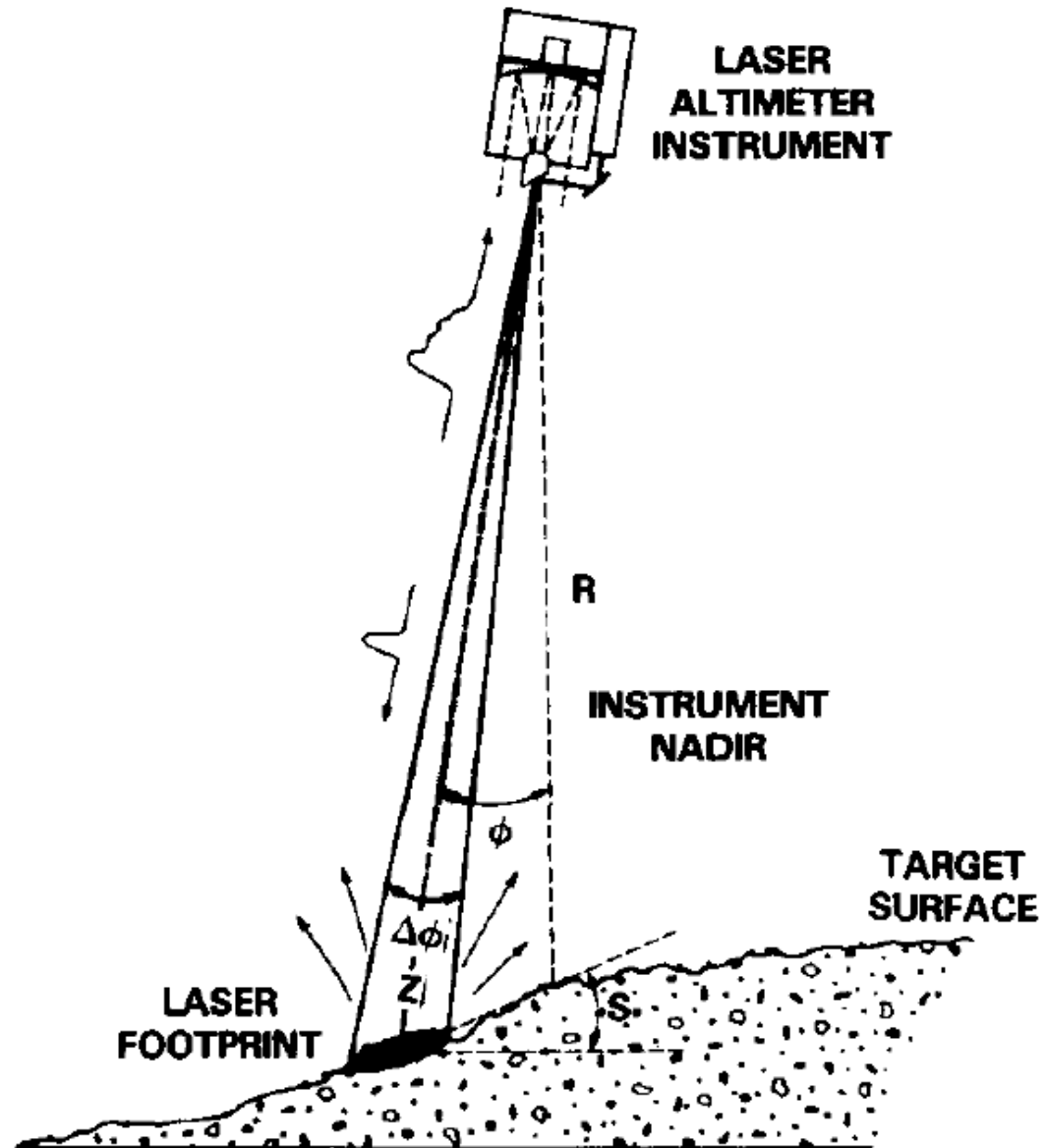
- ❑ Lower atmosphere study poses a great challenge to lidar community, as many factors are involved with each other and make the derivation of precise information on trace gases interested a very complicated procedure.
- ❑ Different techniques have been developed or proposed for solving these problems. The main idea is how to minimize the influence from aerosol backscatter and extinction and how to minimize the interference from other gas molecules. Two major solutions for now: to use Raman scattering to avoid aerosol scattering get into the signal channels, or to use multi-wavelength selection to cancel out the influence from aerosol and other molecules.
- ❑ Other possible ways are to measure several interference gases simultaneously with multiple channels or to combine the DIAL with Doppler lidar etc to study the dynamic transportation of pollutant.
- ❑ The DIAL and Raman lidars are still far from perfection. It could be a growing point in lidar field.

# Motivations to study targets

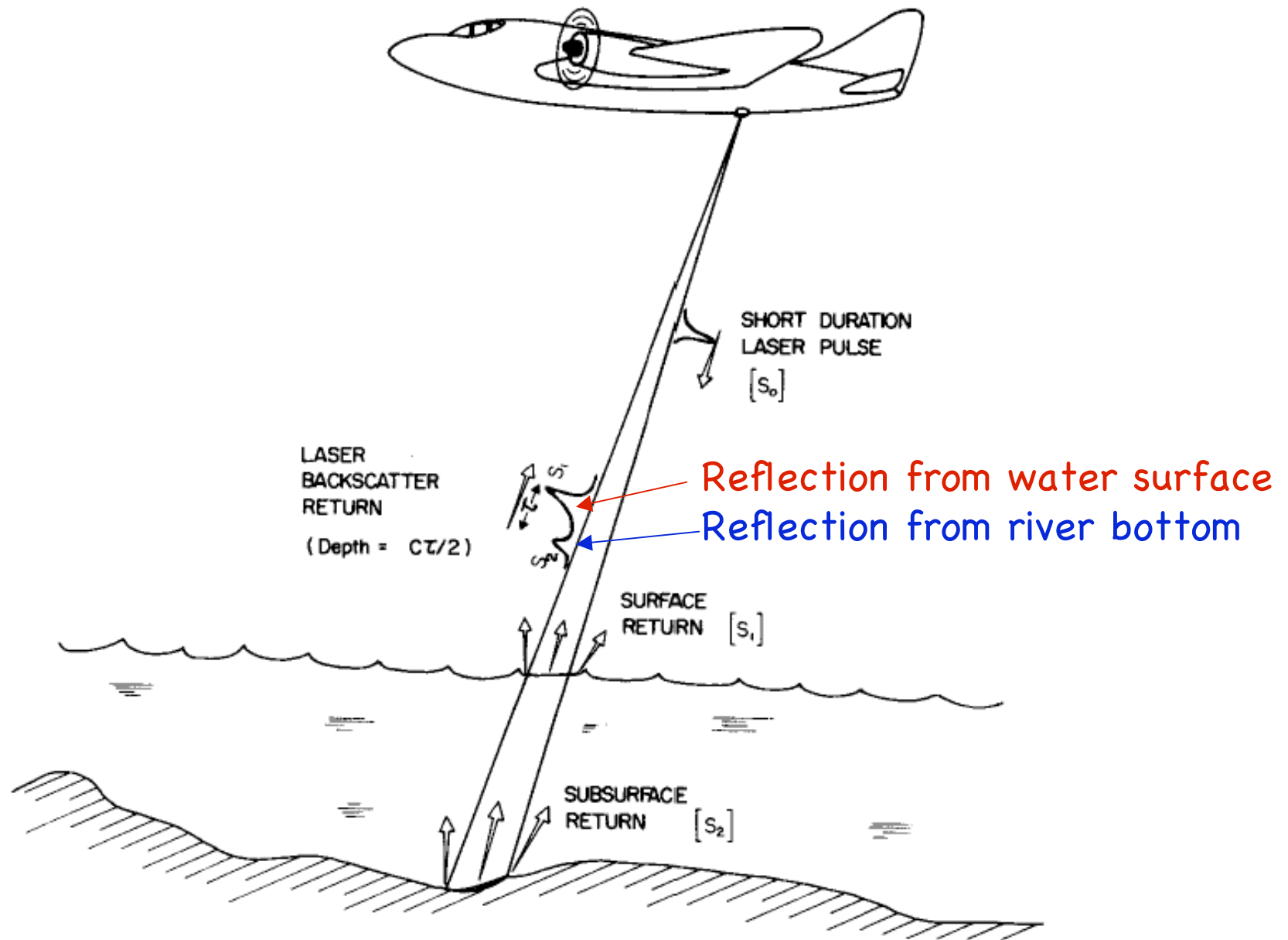
- ❑ What were discussed above are all concerned about atmospheric lidars, with the main purpose to study the atmosphere, and mainly based on the scattering processes (including elastic and inelastic scattering, and absorption and resonance fluorescence) from gas phase atoms, molecules, and aerosols.
- ❑ Besides atmosphere, our environment includes many other things, like the solid earth, cryosphere, hydrosphere, and non-gas-phase objects on the earth, in the ocean, and in the air (e.g., plants, oil, buildings) etc. Study of our environment demands good measurement technology and approach for measurements in all sorts of occasions. Therefore, lidar technology for target (anything other than gas phase objects) detection is essential and highly demanded.
- ❑ Two main categories for target lidars: (1) lidars for ranging (laser altimeter) and (2) lidars for species identification (fluorescence lidar).
- ❑ Laser altimeter - an important approach to monitor sea level, earth and cryosphere surface, military targets for precise range determination
- ❑ Fluorescence lidar - environmental study of hydrosphere, solid earth, cryosphere, plants, oil films on the surface, etc.

# Laser Altimeter (Laser Ranging)

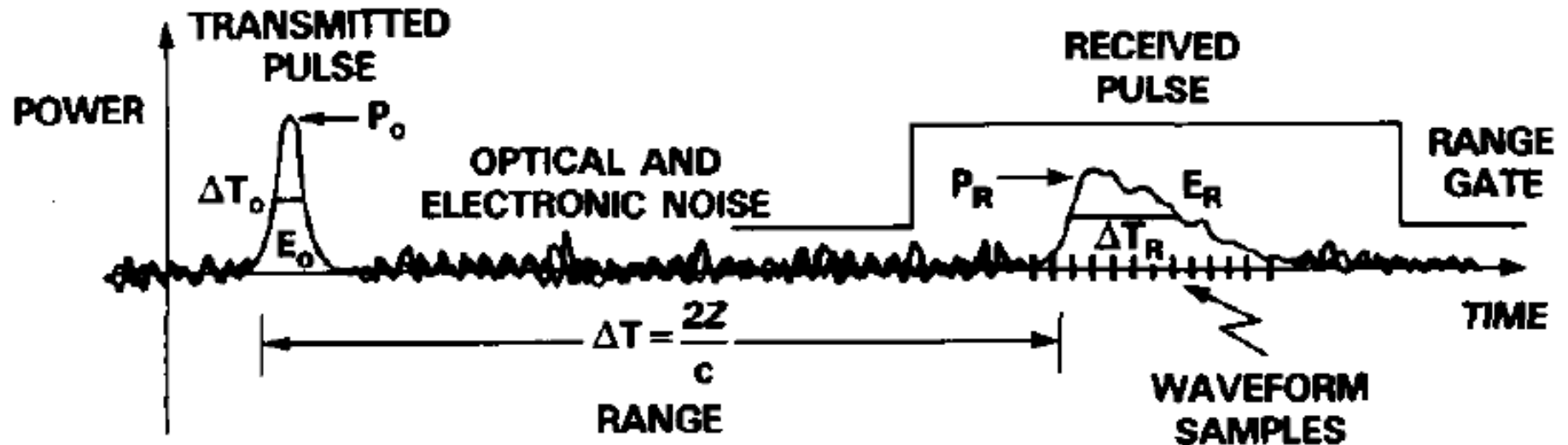
- ❑ The **time-of-flight** information from a lidar system can be used for laser altimetry from airborne or spaceborne platforms to measure the heights of surfaces with high resolution and accuracy.
- ❑ The reflected pulses from the solid surface (earth ground, ice sheet, etc) dominant the return signals, which allow a determination of the time-of-flight to much higher resolution than the pulse duration time.



# Laser Altimeter for Hydrosphere



# Altitude Determination



- ❑ The range resolution is now determined by the resolution of the timer for recording pulses, instead of the pulse duration width. By computing the centroid, the range resolution can be further improved.
- ❑ Altitude accuracy will be determined by the range accuracy/resolution and the knowledge of the platforms where the lidar is on.
- ❑ In addition, interference from aerosols and clouds can also affect the altitude accuracy.

Altitude = Platform Base Altitude - Range  $\pm$  Interference of aerosols and clouds

# Geoscience Laser Altimeter System (GLAS) on the ICESat

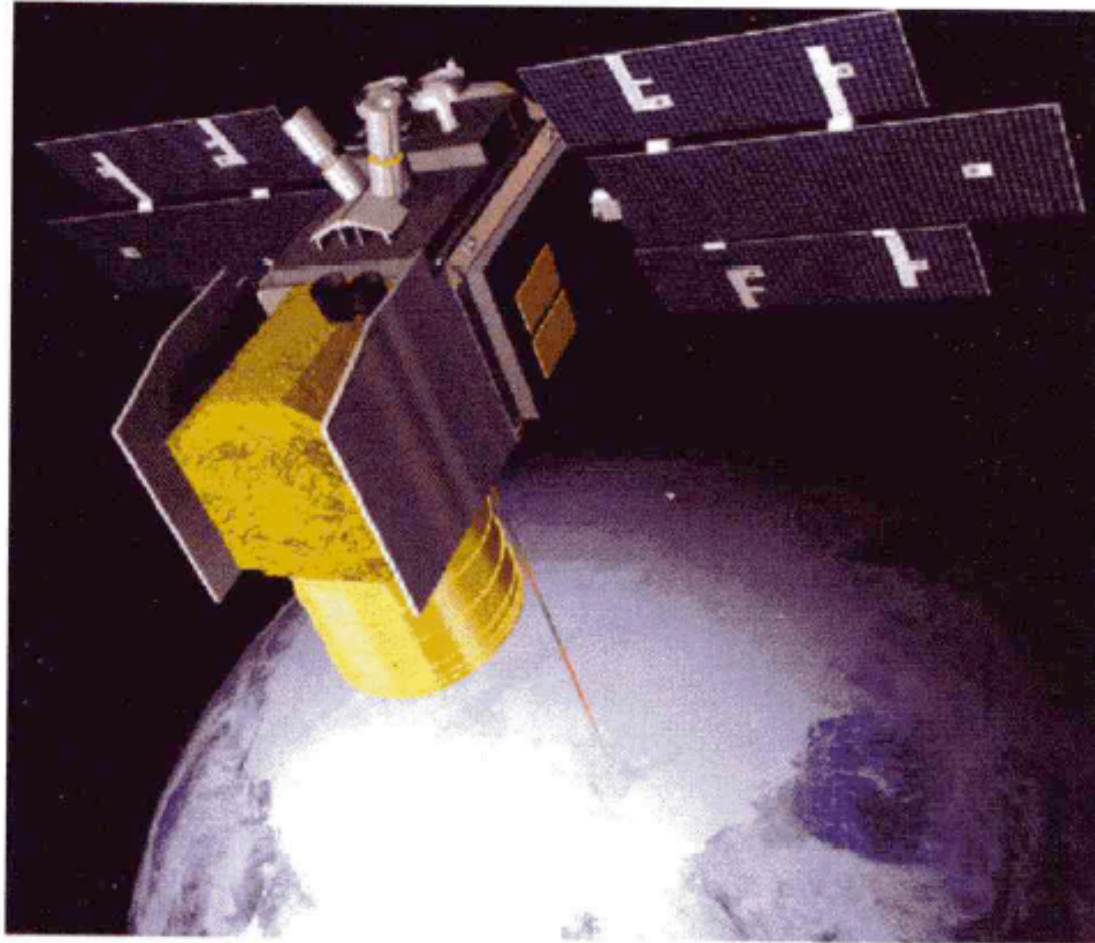


**Fig. 13.23.** An artist's rendition of the ICESat spacecraft with the GLAS instrument onboard. The 1064 nm and 532 nm laser pulses are shown probing the Earth's atmosphere and polar ice thickness changes. (Courtesy of S.P. Palm.)

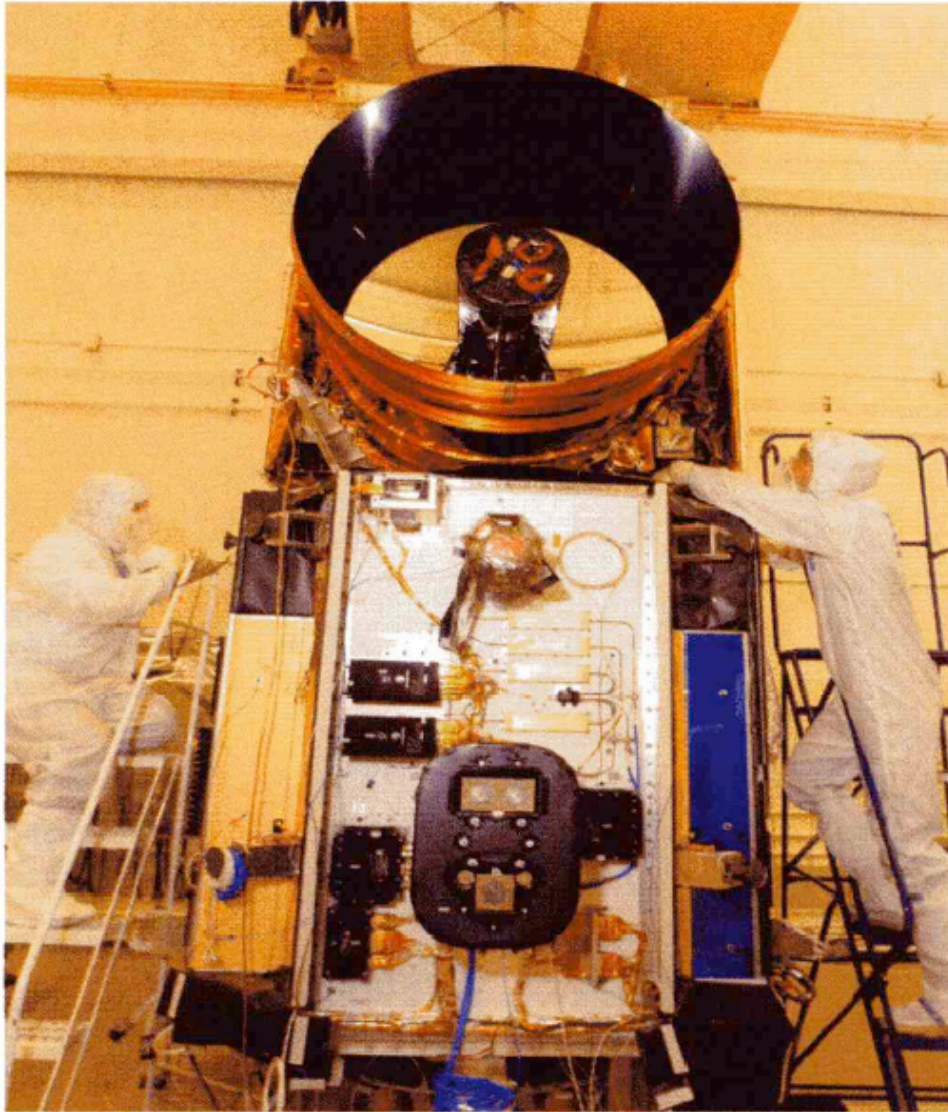
# GLAS Objectives and Specifications

- ❑ The primary purpose of GLAS is to detect ice elevation changes by precision profiling of ice surface elevations over the Greenland and Antarctic ice sheets, that are indicative of changes in ice volume (mass balance) over time.
- ❑ Other objectives include measurements of sea ice, ocean, and land surface elevations; ice, water, and land surface roughness; multiple near-surface canopy heights over land; and cloud and aerosol layer heights.
- ❑ Diode-pumped Nd:YAG laser at 1064 nm for surface topography measurements.
- ❑ Frequency-doubled laser at 532 nm for cloud/aerosol and atmospheric study.

**Table 13.2.** System parameters for the spaceborne GLAS lidar (Courtesy of S.P. Palm.)

Parameter	532-nm Channel	1064-nm Channel
Orbit altitude	600 km	600 km
Laser energy	36 mJ	73 mJ
Laser divergence	110 $\mu$ rad	110 $\mu$ rad
Laser repetition rate	40 Hz	40 Hz
Effective telescope diameter	0.95 m	0.95 m
Receiver field of view	160 $\mu$ rad	475 $\mu$ rad
Detector quantum efficiency	70%	35%
Detector dark current	$3.0 \times 10^{-16}$ A	$50 \times 10^{-12}$ A
RMS detector noise	0.0	$20 \times 10^{-12}$ A
Electrical bandwidth	$1.953 \times 10^6$ Hz	$1.953 \times 10^6$ Hz
Optical filter bandwidth	0.030 nm	1.00 nm
Total optical transmission	30%	55%

# GLAS on ICESat



University of Colorado  
NSIDC is also involved  
in the ICESat.  
(National Snow and  
Ice Data Center)

**Fig. 13.22.** Shows the ICESat during fabrication in a clean room at Ball Aerospace and Technologies Corporation, Boulder, Colorado. ICESat was launched on a Boeing Corporation Delta II launch vehicle, January 2003.

# Challenges in Laser Altimeter

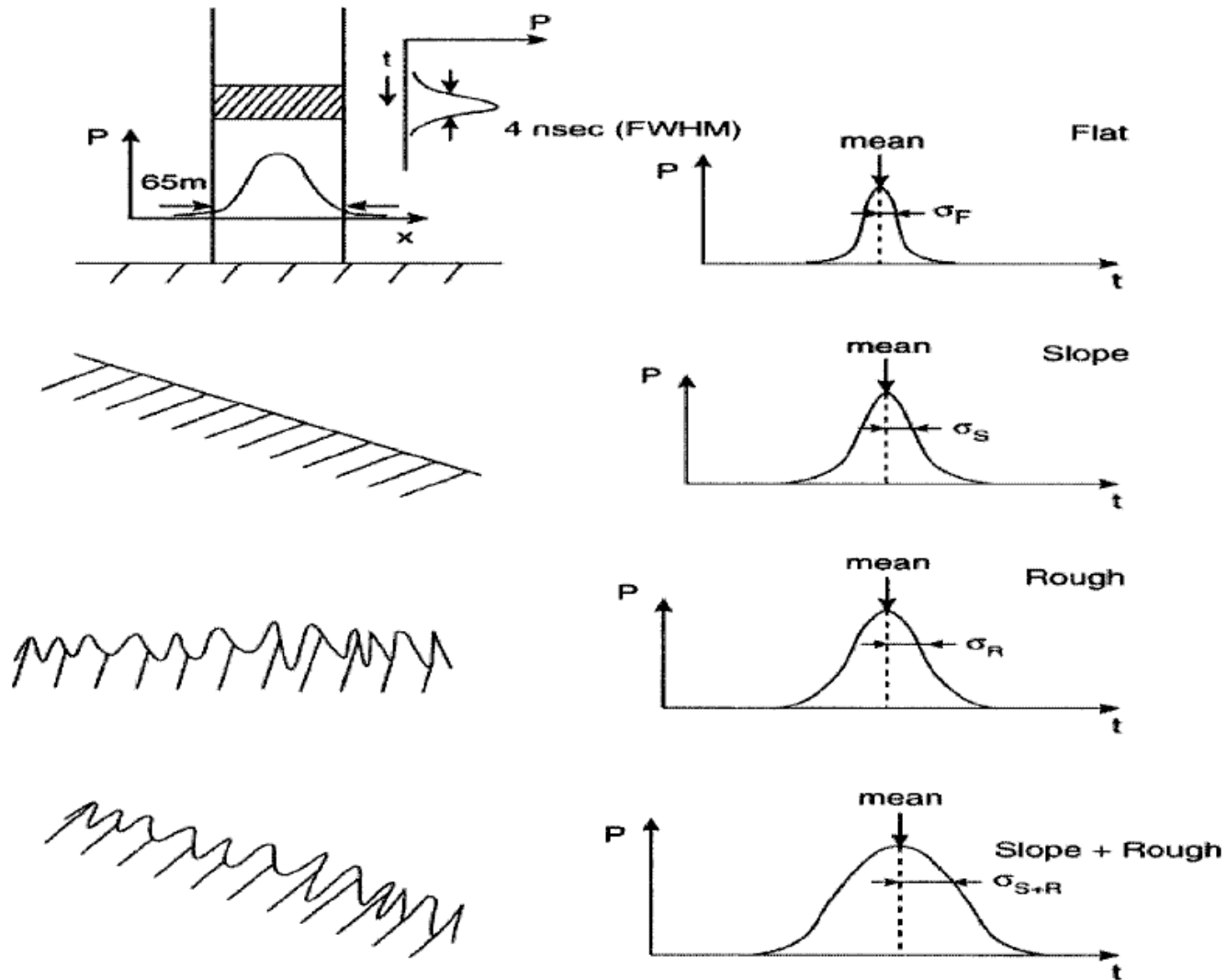
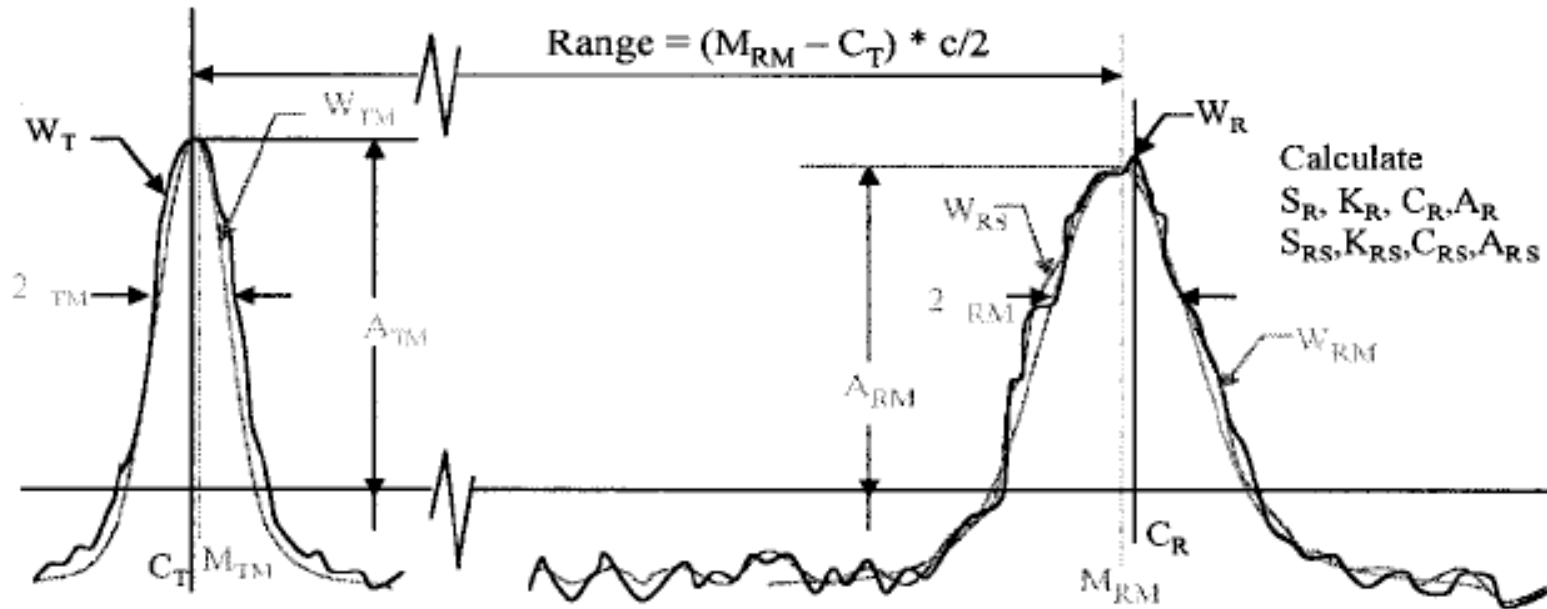


Figure 1 - Characteristics of returned laser pulse as a function of surface type. Presence of surface slope and roughness both broaden the pulse.

# Signal Processing in Altimeter



A - Max Amplitude  
 W - Waveform  
 M - Gaussian Mean  
   - Gaussian 1/e halfwidth  
 C - Centroid (abscissa value)  
 S - Skewness  
 K - Kurtosis

$( )_T$  - Transmitted Pulse  
 $( )_{TM}$  - Model of Transmitted pulse  
 $( )_R$  - Return Pulse  
 $( )_{RM}$  - Model of Return Pulse  
 $( )_{RS}$  - Smoothed Return Puls

**Figure 3 - Characterization of transmitted and received pulse waveforms**

[Brenner et al., GLAS Algorithm Theoretical Basis Document, 2003]

# Other Challenges

❑ Besides the analysis of waveform distortions caused by surface slope and roughness, other factors that can affect the accuracy of laser altimeter include

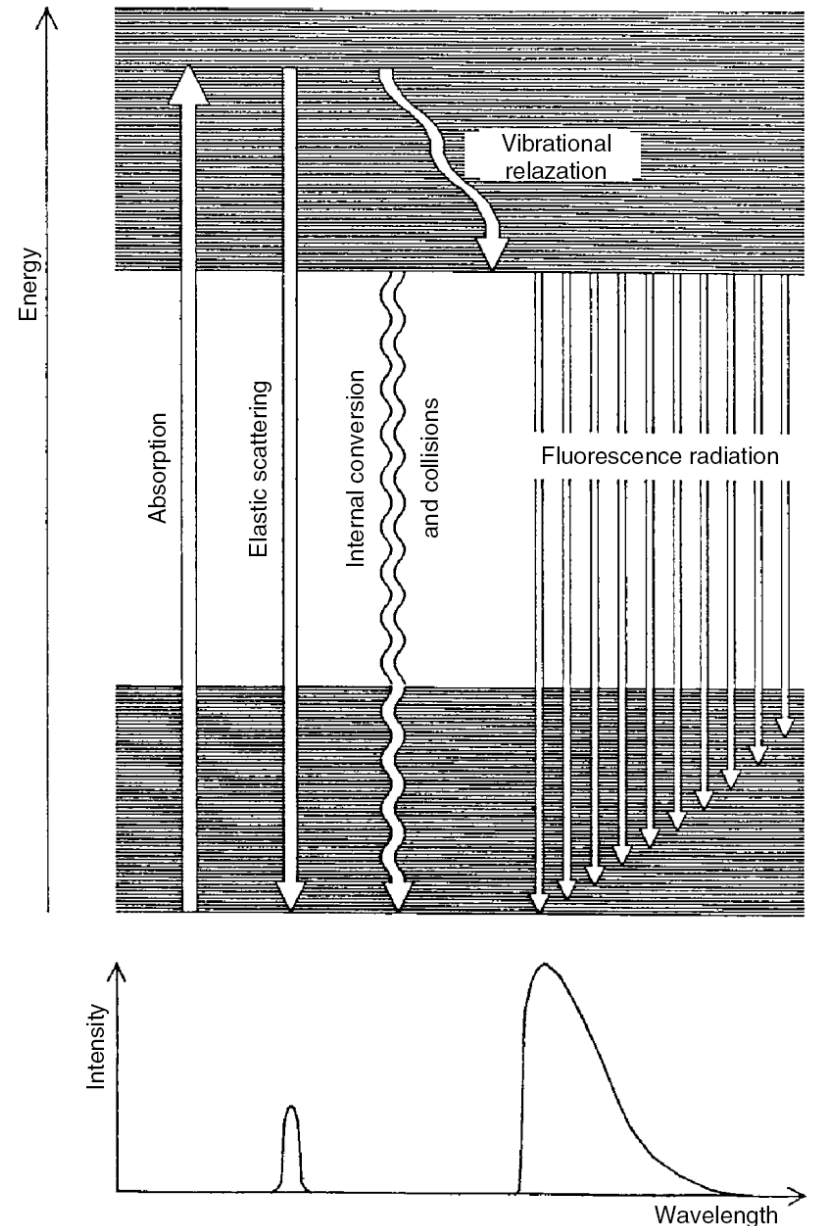
- (1) Orbit and attitude calculations for the platforms
- (2) Corrections for atmospheric path-length delays
- (3) Corrections for changes in the surface elevations due to tidal effects
- (4) Conversion ranges into absolute surface elevations with respect to the geoid.

**Table 9.10** Ice Altimetry Error Budget

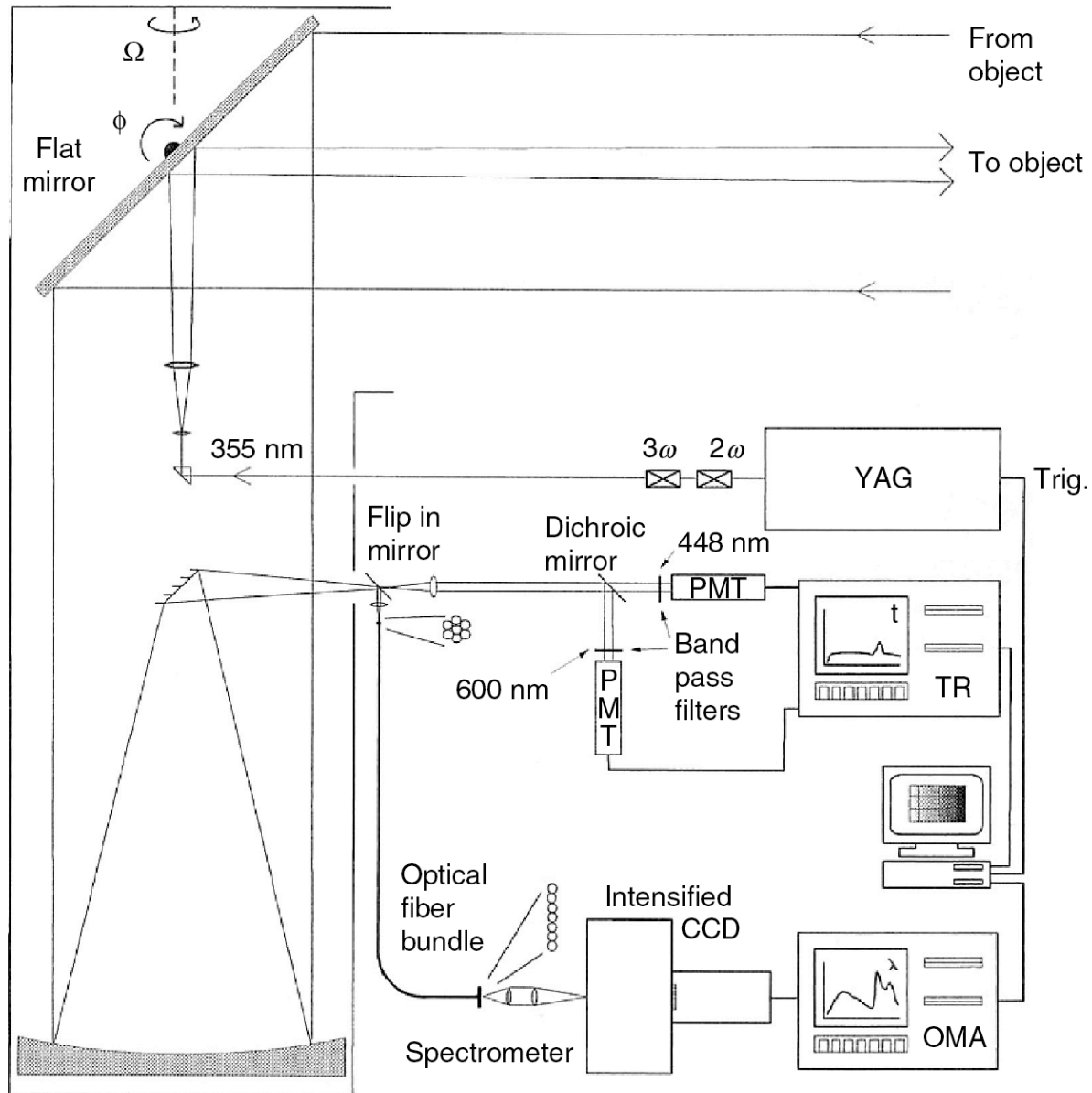
Source	Error type	Magnitude (cm)
Instrument	Single-shot accuracy (3° surface features)	<10
	Range bias	<5
	Laser beam pointing angle uncertainty (1 arcsec, 2° surface)	18
	Radial orbit uncertainty	5
	Clock synchronization (1 μsec)	1
Spacecraft	Distance uncertainty from S/C POD to GLAS zero reference point	0.5
Environment	Atmospheric error (10-mbar error, 0.23 cm/mbar)	2
	RSS error	0.20

# Fluorescence from Liquids and Solids

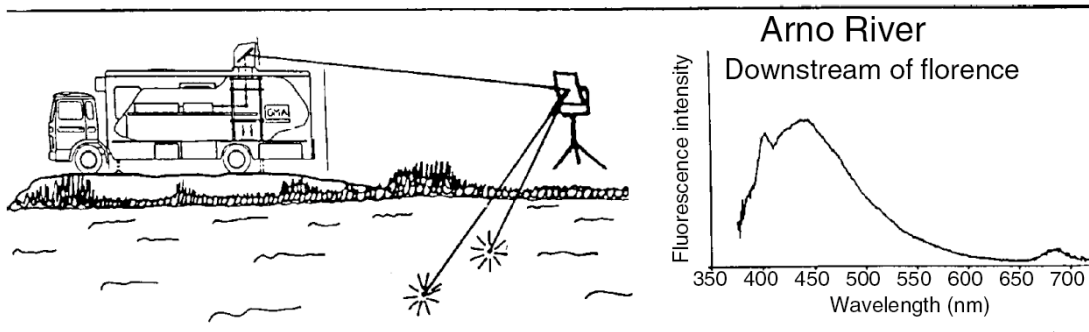
- ❑ In contrast to free atoms and molecules, solids and liquids exhibit broad absorption and emission spectra because of the strong intermolecular interactions.
- ❑ A fixed frequency laser can be used for the excitation due to the broad absorption.
- ❑ Following the excitation, there is a very fast (ps) radiationless relaxation down to the lowest sub-level of the excited state, where the molecules remain for a typical excited-state fluorescence lifetime.
- ❑ The decay then occurs to different sub-levels of the ground state giving rise to a distribution of fluorescence light, which reflect the lower-state level distribution.
- ❑ Fixing the excitation wavelength, we can obtain fluorescence spectra. While fixing the detection channel and varying the excitation wavelength, an excitation spectrum can be recorded.



# Fluorescence Lidar System

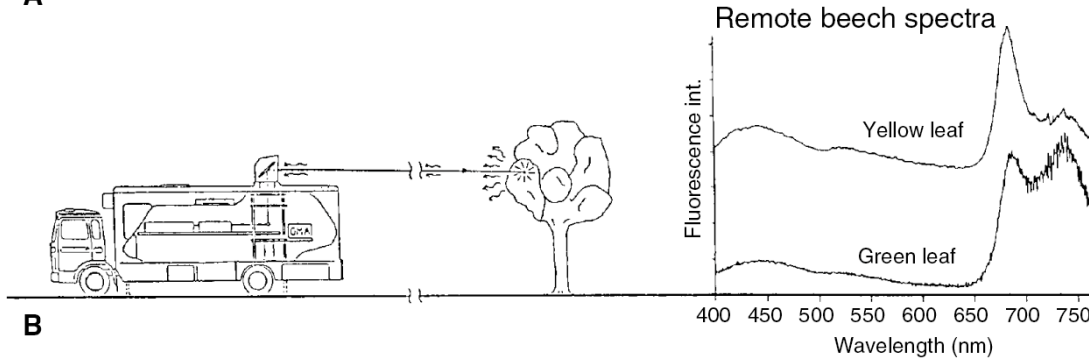


# Scenarios for Fluorescence Lidar



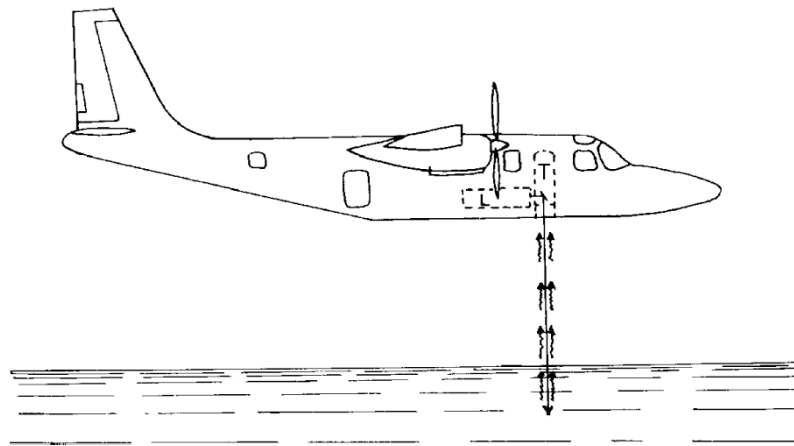
Aquatic monitoring  
Via folding mirror

A



Vegetation  
Monitoring

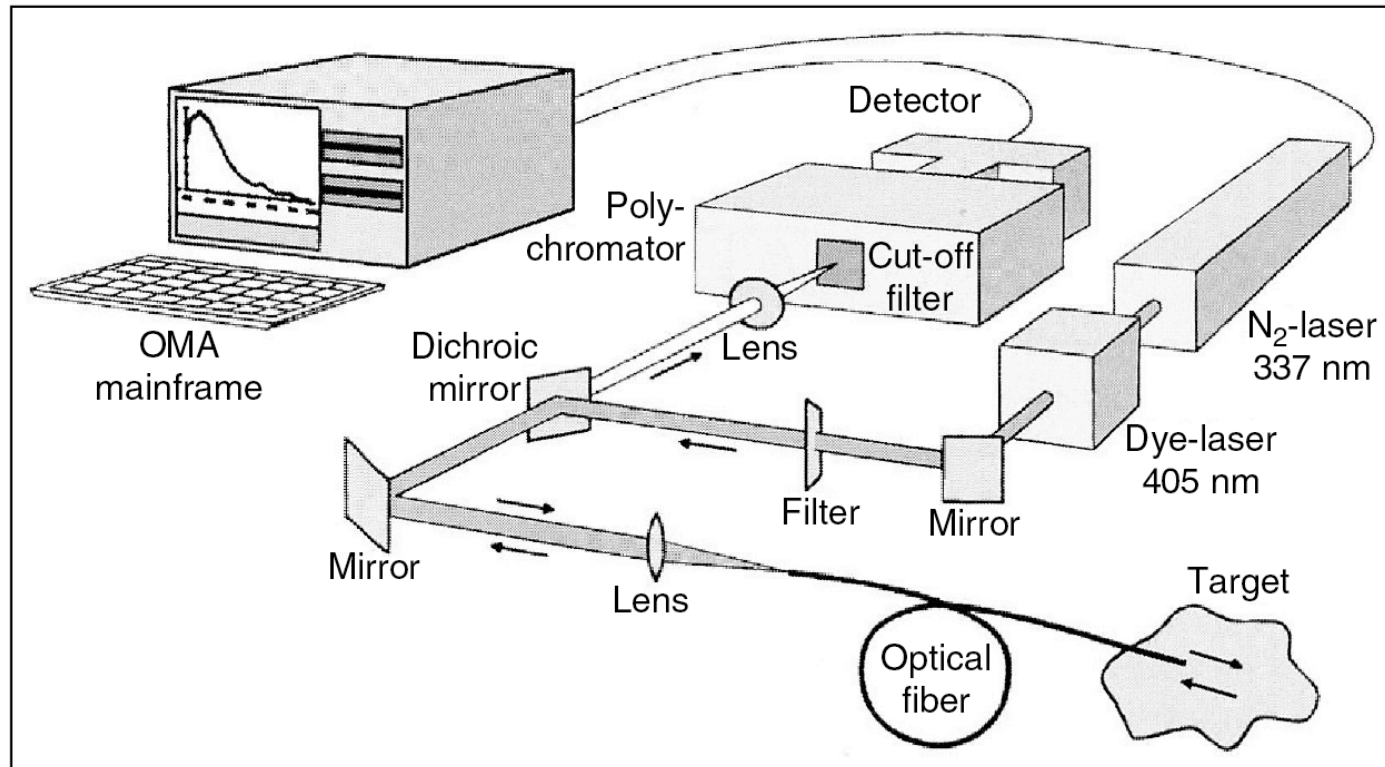
B



Airborne  
Fluorescence

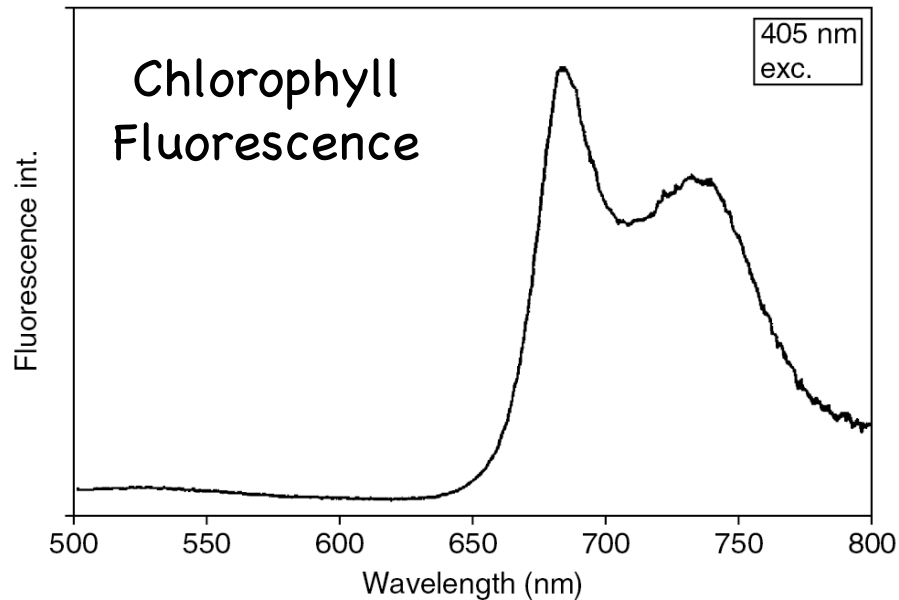
C

# Fluorescence Lidar Setup

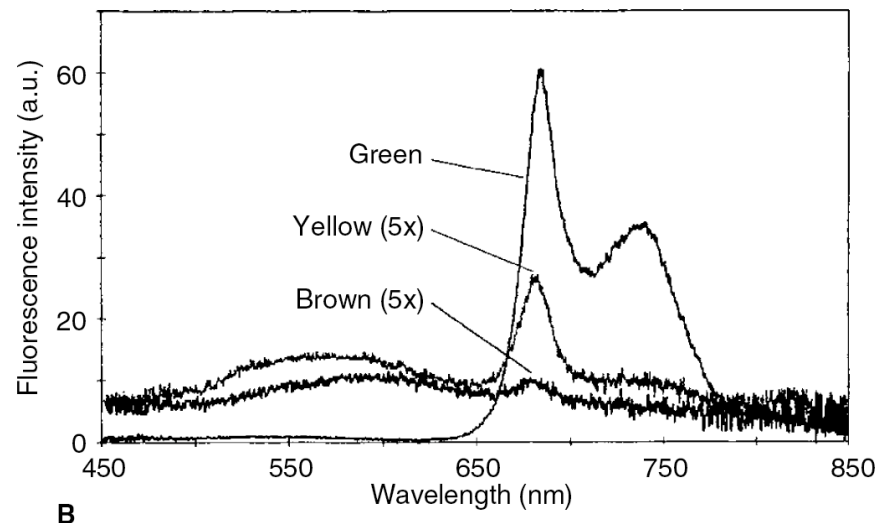
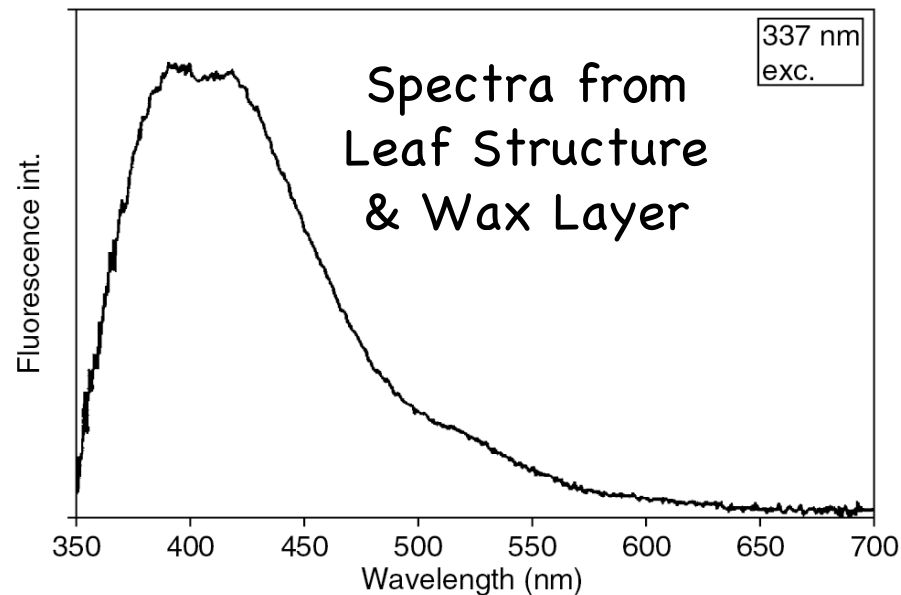


- ❑ Excitation: mainly 337nm from N<sub>2</sub>-laser, or 405 nm from dye-laser
- ❑ Fiber: transmit laser pulse and collect laser-induced-fluorescence
- ❑ Filters: Dichroic mirror reflect laser light and transmitting red-shifted fluorescence; cut-off filter further reducing background
- ❑ Time-gating: only accept light during a narrow time window after certain time of the transmitted pulse - efficiently eliminate background light
- ❑ Detector: spectrometer + CCD to record full spectrum covering 350-800 nm following each laser shot

# Vegetation Monitoring

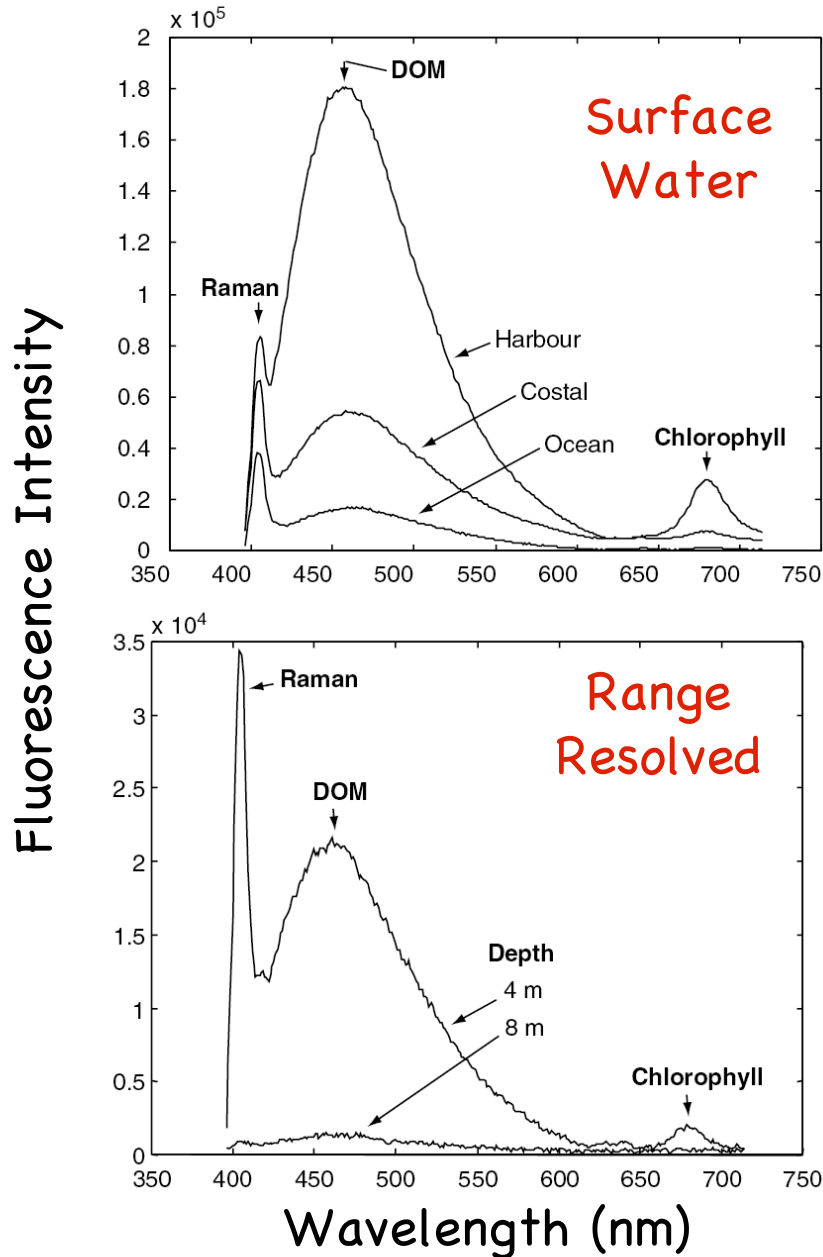


- When excited by 405 nm, the chlorophyll fluorescence is clearly visible with peaks at 690 and 735 nm. This also means that chlorophyll has strong absorption at the red spectra.
- When excited by 337 nm, the fluorescence from wax layer is strong in the blue spectra, while protection layer prevents the penetration of UV light reaching chlorophyll.



Signals from different leaves

# Marine Monitoring



- ❑ Excitation at 355 nm
- ❑ Raman scattering from  $H_2O$  at 404 nm (Raman shift:  $3400\text{ cm}^{-1}$ ) - Because the aggregation of water molecules depends on the temperature, the analysis of the detailed shape of the Raman signal can be utilized to measure surface water temperature.
- ❑ DOM (Dissolved Organic Matter) fluorescence in the blue-green spectral region for assessment of the general level of DOM.
- ❑ By normalizing the DOM signal to the bkg-free water Raman signal, the percentage of DOM in water can be derived (a built-in reference).
- ❑ Range-resolved fluorescence data can be taken by gating the image intensifier at different delays.

# Detection of Historic Monument

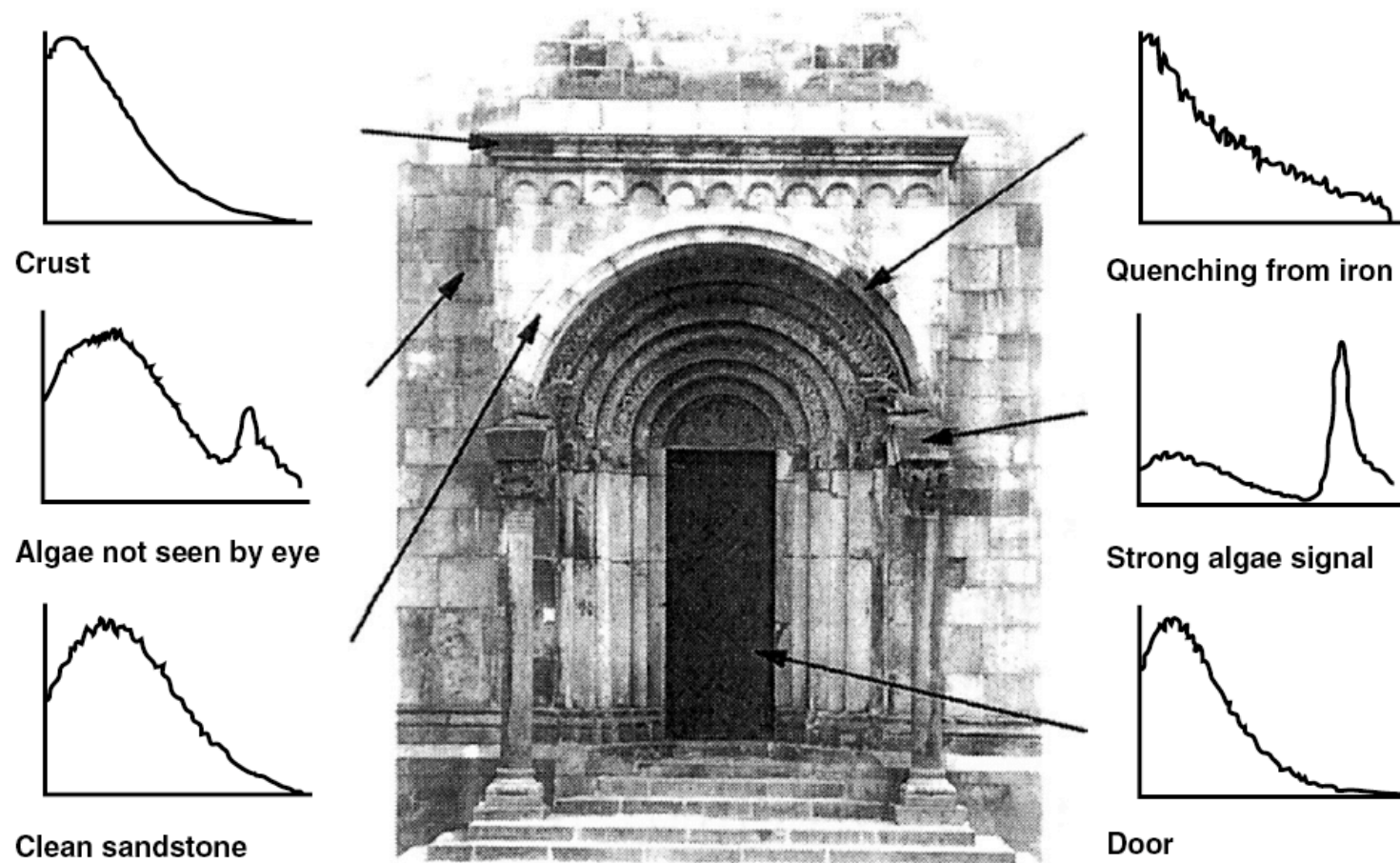


**Figure 6.13** Photograph of the northern gate of the Lund Cathedral and six remotely recorded fluorescence spectra. (From Weibring, P. et al., *Appl. Opt.*, 40, 6111, 2001. With permission.)

# More Target Lidar & Imaging Lidar

- ❑ Besides laser altimeter and fluorescence lidar, other target lidars include the lidars for detecting fish school (fish lidar, NOAA), for detecting vibrations (Coherent Technologies, Inc), for detecting or imaging buildings, military targets, airplanes, etc.
- ❑ They all utilize the time-of-flight between the reflected laser pulses or light from the targets and the transmitted laser pulse to determine the positions (range or 3-D spatial position) of targets.
- ❑ The scanning type of target lidars is sometimes called "ladar", meaning "laser radar". Utah State University has a group doing ladar business.
- ❑ By scanning fluorescence lidars, the mapping of ocean surface or plant distributions can be obtained.
- ❑ Airborne and spaceborne lidars, especially the laser altimeter and fluorescence lidar, have found wide application range and usefulness.
- ❑ Compact laser altimeter aboard Unmanned Aerospace Vehicle (UAV) has promise applications. Aerospace faculty James Maslanik and Brian Argrow are leading the effort of laser altimeter on UAV.

# Summary of Target Lidar

- ❑ Target lidars, including laser altimeter, hydrosphere lidar, fluorescence lidar, ladar, fish lidar, etc, are an variant of atmospheric lidars. They share some of the same techniques used in atmospheric lidars.
- ❑ Laser altimeter and ladar use time-of-flight to determine the range of objects or surface. Many factors are involved.
- ❑ Fluorescence is used to measure organic materials, plants.
- ❑ Raman scattering by water is used to normalize the lidar returns.
- ❑ Target lidars face some different challenges and difficulties than atmospheric lidars. These challenges and difficulties also determines the growing points in this field.
- ❑ Target lidars have been deployed on different platforms for various applications. More efficient and compact target lidars on platforms like UAV, promise more applications.